National University of Science and Technology
POLITEHNICA of Bucharest
Faculty of Mechanical Engineering and Mechatronics
Department of Therodynamics, Thermal Engines and Refrigeration Equipment

DOCTORAL THESIS ABSTRACT

Theoretical and experimental study regarding the use of phase change materials in the refrigeration systems defrosting

Author: Eng. AL DOURI Jamal F.M.K.

PhD supervisor: Prof. Dr. Eng. Tudor PRISECARU

DOCTORAL COMMISSION

President	Prof. Dr. Eng. Camelia STANCIU	from	POLITEHNICA Bucharest
Coordinator	Prof. Dr. Eng. Tudor PRISECARU	from	POLITEHNICA Bucharest
Member	Prof. Dr. Eng. Alexandru SERBAN	from	POLITEHNICA Bucharest
Member	Prof. Dr. Eng. Gabriel NASTASE	from	Transilvania University of Brașov.
Member	Conf. Dr. Eng. Ema Carmen PANAITE	from	Gheorghe Asachi Technical University of Iași

Bucharest
2026

ACKNOWLEDGEMENTS

Above all, I wish to thank God for everything.
I would like to thank Prof. Dr Eng. **Tudor PRISECARU,**
I would like to extend my heartfelt appreciation to my primary advisor, Professor Dr. Eng. **Valentin APOSTOL**, for his unwavering support throughout my doctoral studies and research endeavors. I am grateful for his patience, encouragement, excitement, and extensive expertise in the field. The mentor's assistance was invaluable throughout the whole duration of the research and writing process for this thesis. I could not have envisioned a more exceptional adviser and mentor for the duration of my doctoral studies.
I would like to thank my special appreciation and thanks to my co-supervisors Dr Eng. **Horațiu POP and Claudia IONIȚĂ**, for his encouragement, insightful comments, and challenging questions, as well as his valuable and fundamental contribution, which was represented in the continuous financial support for the provision of the experiment equipment and control panel preparation, as well as valuable advice and guidance to achieve the desired objectives of this work.
In the experimental direction, I would like to thank the technicians, **Laurentiu Gheoldea, Mircea Hera and Eugen Georgescu** for their wonderful help with the experimental set-up.
I owe a big debt of gratitude to my amazing **wife**, my children (**Ahmed**, **Aye** and **Dania**) and my brother prof**. Ing. KHALIL Hisham** who worked tirelessly alongside me and our family in order to finish and fulfill the requirements of this thesis.
I would like to thank all my **friends**.

Tabel of Contents

Tabel of Contents 3
1 Chapter 1 5
Introduction 5
1.1 Vapour compression refrigeration system (VCRS) 6
1.2 The main components of the VCR cycle 6
1.3 Vapour compression refrigeration cycle 6
Conclusion 7
2 Chapter 2 8
Literature review regarding methods to enhance the efficiency of VCRs 8
2.1 Compressor performance enhancement methods 8
2.1.1 Addition of nanoparticles in the lubrication oil 8
2.1.2 Using phase change materials (PCMs) 8
2.2. Condenser performance enhancement methods 8
2.2.1. The effect of shading on the condenser 8
2.2.2. The effect of evaporative condensers 8
2.2.3. The effect of subcooling 8
2.3. Expansion valve performance enhancement methods 8
2.4. Evaporator performance enhancement methods 9
2.4.1. Passive defrosting methods 9
2.4.2. Active defrosting methods 9
2.4.3. Methods of defrosting based on PCMs 10
2.5. Heat recovery to enhance the efficiency of VCRS 10
2.6. Enhancement of VCRs efficiency using PCM 10
2.6.1. Characteristics and classification of phase change materials (PCMs) 10
2.6.2. Researches for enhancement methods the adding PCM in the refrigeration system 11
3 Chapter 3 12
Study regarding the use of PCMs for the defrost of VCRs considering multiple refrigerants 13
3.1 Mode of operation of VCRs by Incorporating Phase Change Materials 12
3.2 Refrigeration Cycle on a p-h Diagram of VCRs by Incorporating Phase Change Materials 12
3.3 Modelling of the PCMs defrost refrigeration system 13
3.4. Results and Discussions 14
4 Chapter 4 16
Experimental Analysis of Air or Electric Heater Defrosting in a VCRS 13
4.1 Experimental rig 16
4.1.1. Evaporator (Eva) 16
4.1.2. Compressor (Cp) 16
4.1.3. Condenser (Cd) 16
4.1.4. Expansion valve (E.v) 17
4.2 Results and discussion 17
5 Chapter 5 20
Experimental Study of PCM for Thermal Energy Storage 20
5.1 Experimental rig 20

5.1.1 Test section 20
5.1.2 Auxiliary equipment 21
5.1.2.1 Hot water vessel 21
5.1.3.1 Temperature sensor 21
5.1.3.2 Flow meter water 22
5.1.3.3 Stopwatch 22
5.1.3 Measurement Devices 21
5.2. Results and discussion 22
Chapter 6 27
Comparison between defrosting methods using different refrigerants 27
6.1 Introduction 27
6.2 The mathematical model of a VCRS with defrosting process 27
6.2.1 The mathematical model for VCRS air defrosting 29
6.2.2 The mathematical model for VCRS electric heater defrosting 29
6.2.3 The mathematical model for VCRS hot gas defrosting 30
6.2.4 The mathematical model for VCRS PCM defrosting 31
6.3 Results and discussion 32
Chapter 7 36
Conclusions and personal contributions 36
C.1. General conclusions 36
C.2. Original contribution 39
C.3. Future research direction 40
Published articles 42
Selective Bibliography 43

Chapter 1
Introduction

As the world economy has grown, there has been a huge rise in the need for electricity. Energy shortages are a major concern for the future development of the planet, and at the same time, the growing population causes the need for more energy to provide for their needs, which necessitates more energy production [1]. The increase in energy consumption causes increases in the emission of toxic gases into the atmosphere, especially carbon dioxide (CO_2), which is one of the causes of pollution and climate change [2].The latest conference on climate change organized by the United Nations was held in Sharm el-Sheikh., which was published in data on November 20, 2022, placed a strong emphasis on carbon dioxide, which is the principal cause of rising temperatures globally, resulting in an annual increase of about 0.5 °C [3].

R and AC systems utilize around 30% of the electrical energy consumed. In many countries, researchers are interested in developing refrigeration systems for reducing energy consumption, not only by optimizing energy utilization but also by lowering consumption without affecting comfort or other benefits related to energy consumption or affecting installation efficiency or quality [11],[12].

The defrost system is an essential component in RS that consumes a significant amount of electricity. One of the most serious issues with VCRs in many applications, such as household and HP is the production of frost on Eva surfaces [13]. When the temperatures of the Freon reach a negative value in the Eva pipe, the water vapor in the air condenses, freezes and gradually forms a frost layer on the Eva pipe. The disadvantages of frost accumulation are:

a) Reduce the heat transfer: Frost acts as a thermal insulator, which decreases the heat transfer between the Eva surface and the surrounding air. This can lead to a reduction in cooling capacity and at the same time lead to increasing in the time of cooling cycles [3];
b) Increases power consumption: As the frost layer becomes thicker, the refrigeration system must work harder to maintain the desired temperature, and this causes a higher energy consumption [14];
c) Reduction of the airflow in the Eva: When frost accumulates, it can block the airflow in the Eva, reducing the amount of air that passes through the fins. This can decrease heat exchange and efficiency, causing the refrigeration system to work harder;

Taking into account all the above mentioned factors, the performance coefficient of the refrigeration system will decrease.

The necessity to find new ways to reduce electricity consumption has become essential, and one of the new important methods is TES technology. To make TES economical and sustainable, several researches have been done on its crucial components. TES has significant promise as a technological solution that may effectively enable the shift of energy use from high-demand to low-demand periods of time [3]. Application areas for TES technology include solar energy, AC, construction, etc. TES may be divided into three main methodologies: sensible-heat storage, latent- heat storage and thermochemical. PCM is widely utilized because of its amazing benefits, including improved TES and the capacity to effectively store and release a substantial amount of energy at a constant temperature via the charging (melting) and discharging (solidification) processes [15]. The energy is accumulated during the phase transition of melting and then released during the solidification process [16].

A refrigeration system operates in two stages: a cold stage that removes heat, and a defrosting stage that melts ice from the evaporator surface. If the ice isn't removed, it would reduce the system's efficiency and increase energy consumption. The total energy consumption of the refrigeration system includes two components: energy consumption during defrosting and energy consumption during cooling operation. In calculating overall energy consumption, we allocate values to each component based on the duration of operation in cooling mode relative to defrost mode, whichever defrosting method is used.

1.1. Vapour compression refrigeration system (VCRS)

Since the discovery of VCRS at the beginning of the 19th century, VCRs have been extensively used in different types of household refrigerators, industrial freezers, and air conditioning [11].The vapor compression refrigeration cycle, during process evaporation, take heat from low temperatures and rejects heat from high temperatures to the environment during process condensation. Schematically Figure 1.4 depicts the VCR's four key components: The Cp, Con, Ev, and Eva, through which the refrigerant flows in a closed loop [17]. The VCR system is based on thermodynamics' second law. According to this statement, "It is impossible to transfer heat from a low-temperature body to a high-temperature body without the application of external force" [18]. Refrigeration systems, the standard residential and industrial devices, are widely used to transfer heat between different locations. The working principle of most RS is based on VCR. Refrigerant(R) fluid boils at low temperatures in the Eva as it absorbs heat during boiling or evaporation, and then is removed at high temperatures in the surrounding environment in the condenser [19],[20].

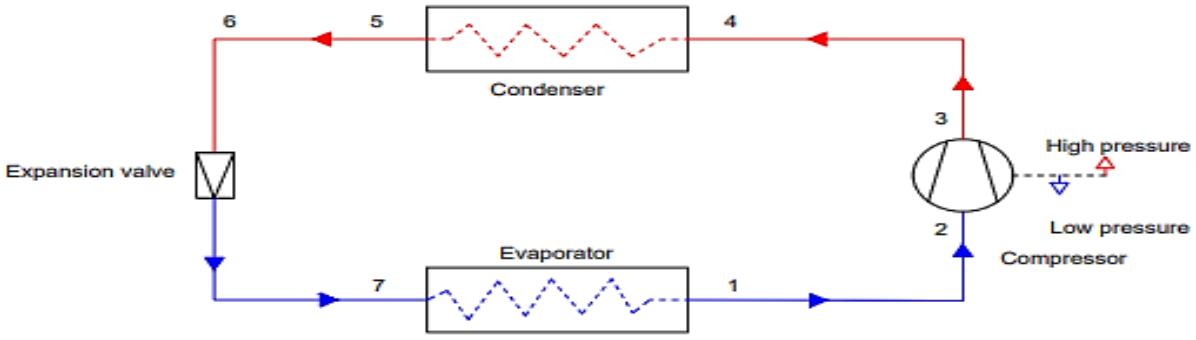


Figure 1.1 Components of VCR cycle

1.2 The main components of the VCR cycle

The VCR is composed of four main parts: the Cp, Con, Ev, and Eva, which function inside a closed loop system as in Figure 1.1

1.3 Vapour compression refrigeration cycle

There are four main steps in the refrigeration cycle. The expansion device's isenthalpic pressure decreases, the Cp's isentropic compression, the Con's isobaric heat rejection, and the Eva's isobaric heat addition. The traditional VCR cycle used in the analysis for the VCR system with superheating and subcooling is shown in Figure 1.2.

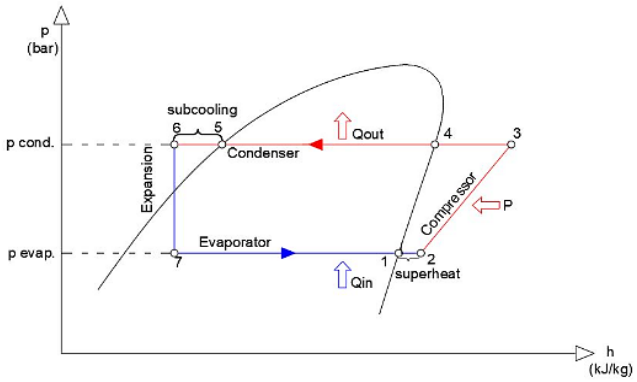


Figure 1.2 p-h diagram for the thermodynamic VCR

Conclusion:

Globally the VCRSs are important energy consumers. One of the interesting strategies for enhancing the installation's performance is to minimize energy consumption during the defrost stage.

In the next chapter a literature review regarding methods to enhance the efficiency of VCRs is conducted.

Chapter 2

Literature review regarding methods to enhance the efficiency of VCRs

2.1 Compressor performance enhancement methods

The Compressor is a key component that consum a lot of energy [23], [24], [25] and should be upgraded. Several researchers are working on ways to enhance the Compressor, one of which is to use nanoparticles, or PCM.

2.1.1 Addition of nanoparticles in the lubrication oil

Increasing the quantity of nanoparticles present in the lubricating fluid is a crucial step toward improving the efficiency of the Cp. Due to the numerous benefits of their properties, such as higher conductivity, lower density and so on, which have allowed them to be used in various parts of the refrigeration system.

2.1.2 Using phase change materials (PCMs)

Liu et al. [34] created a bypass cycle defrosting system for residence refrigeration systems. This system made use of thermal storage in the Cp casing, and it was compared to a normal defrost system that included a heater. The experiment demonstrated that the amount of time needed to defrost had decreased between 65% –77%, the amount of energy used was reduced between 89% – 92%, and the noise level of the Cp was reduced by about 18.5%

2.2. Condenser performance enhancement methods

2.2.1. The effect of shading on the condenser

The AC system consumes a lot of electricity in warm climates. Therefore, Shading a space is one way to lessen the cooling demand and protect against intense sun radiation.

2.2.2. The effect of evaporative condensers

The reduction of energy consumption is a matter of most importance for VCR systems, especially in regions characterized by high temperatures. The enhancement of energy efficiency in a system may be achieved by the improvement of heat rejection from the Con by using evaporative condensers.

2.2.3. The effect of subcooling

In conventional VCR systems, it is often accepted that the refrigerant reaching the Eva is typically regarded as wet vapour. Subcooling the saturated liquid at the condenser exit increases the COP.

2.3. Expansion valve performance enhancement methods

The VCR system is one of the most prevalent types of cooling systems. One of the methods to improve the refrigeration system is to reduce throttling losses by replacing an E.v with an ejector expansion.

2.4. Evaporator performance enhancement methods

Refrigeration and AC systems depend on Evas to absorb heat from cooling room environment and convert refrigerant from liquid to vapor. For this, the formation of frost in refrigeration systems becomes an unavoidable phenomenon. Previous studies have shown that the existence of deposition on the Eva's surface significantly hampers the system's efficiency [1-3]. For all mentioned above defrosting is an important method to enhance Eva performance.

Defrosting methods

There are two main methods for defrosting: passive and active.

2.4.1. Passive defrosting methods

Passive defrosting technologies do not use direct energy during the defrosting process. The most common passive defrost techniques are surface coating and off-cycle defrosting [50].

- **Surface coating defrost method**

In recent years, advancements in material technology have simplified and improved the effectiveness of Eva surface coating as an anti-frosting technique. Studies have demonstrated that the surface coating applied to the Eva surface can slow down the formation of frost on the Eva surface [51], [52]

- **Method of Off – cycle defrost**

In the techniques for off-cycle defrosting, heat is generated from the air around the Eva. As a result, this technique may be used to thaw objects in surroundings with temperatures greater than 1 °C.

2.4.2. Active defrosting methods

Active defrosting involves using external energy sources or mechanical processes to accelerate the defrosting process. The widely used active defrost methods include reverse cycle, ultrasonic vibration, hot gas, electric heating and hot fluid defrosting [50], [52].

- **Method of air defrost (Off – cycle defrost)**

In this case, when the refrigeration system requires defrosting, the Eva fan starts circulating air from the refrigeration room, which has a temperature above 0°C. This recirculation of air causes the defrost accumulated on the surface of the Eva to gradually melt away.

- **Method of reverse cycle defrosting**

The reverse cycle defrost method, is a common technique used in heat pumps, refrigeration, and AC systems to remove frost the accumulates on the outdoor heat exchanger or Eva.

- **Ultrasonic vibration defrost method**

Ultrasonic defrosting uses ultrasonic frequencies [60]. generally, over 20 kHz, to produce vibrations in materials where frost accumulates. The vibrations generate micro motions that allow it to break up frost that form on surfaces Eva coils, without the need for source of heat to melt it.

- **Method of hot – gas defrost**

The hot gas defrost method is a common technique used in refrigeration systems to melt the frost that accumulates on the Eva coil. A tube connects from Cp to the Eva for the defrosting process using the hot-gas method.

- **Electric resistance heating defrost method**

The electric resistance heating defrost method is commonly used in both household refrigerators and large industrial systems to melt the frost that accumulates on the Eva coil. This method depends on electric resistances that generate heat when provided with electrical energy, which is then used to melt the frost on the coil.

- **Hot fluid (water) defrost method**

The hot fluid (water) defrost method is commonly used in refrigeration systems to melt frost that accumulates on the Eva coil. This method works by circulating warm liquid, usually water, through a separate circuit that is connected to the Eva coil.

2.4.3. Methods of defrosting based on PCMs

The use of heat exchangers with PCM to store heat for defrosting has been more interesting in recent years. PCM-based defrosting works by storing thermal energy in the PCM during normal VCRS operation, and then using that stored heat to melt the frost on the Eva coil during the defrost cycle.

2.5. Heat recovery to enhance the efficiency of VCRS

When the system rejects heat for the environment, this is called waste heat. Therefore, we can define waste heat as the energy generated during heat transfer processes such as conduction, radiation, and convection between different components of a RS.

2.6. Enhancement of VCRs efficiency using PCM

The application of PCM in refrigeration systems to improve their efficiency is a novel approach to reducing energy consumption, due to its inherent advantages. The desired characteristics include a high latent heat change, low volume change coefficient, low supercooling, absence of corrosion, strong chemical stability during melting or solidification, low cost, non-toxicity, non-flammability, and high solid and liquid densities [89].

2.6.1. Characteristics and classification of phase change materials (PCMs)

Researchers have become more interested in phase change materials (PCMs) in recent years because of:

- Large capacity for storing energy;
- Storage space is low;
- During the charging and discharging stages, isothermal behavior occurs [102].

The PCMs are able to accumulate or release large quantities of energy at a constant temperature though a change of phase [103].

Phase change materials classification

Classifying PCMs by their melting temperature is essential for determining their suitability for specific applications. Low-temperature less than 15 °C PCMs are commonly used in air conditioning and storage food industry, medium-temperature PCMs between 15-90°C are commonly widely applied in heat load and solar heating and while high-temperature PCMsmore than 90 °C are ideal for absorption refrigeration and industrial heat storage and concentrated solar power [122]

I. Inorganic PCMs

Inorganic PCM has a broad range of melting temperatures, spanning from 10 °C to 900 °C.

Salt Hydrates

Salt hydrates, consisting of a combination of water and salt, are widely recognized as the biggest and most extensively studied kind of hydrates. The melting temperatures of these substances exhibit a range spanning from 15 °C to 117 °C.

II. Organic PCMs

Organic PCMs are often used in a wide range of applications. Which has melting point ranges from 35 to 70 °C

Paraffin

- The chemical formula for paraffin is CH_3-(CH_2)-CH_3. Which has High melting point, no reaction chemically and safe with non-reactive.

Fatty acids

The formula chemical is $CH_3(CH_2)$ 2nCOOH, resemble paraffin in its characteristics. Fatty acids' speedier phase change is their principal benefit. They are somewhat corrosive and more expensive than paraffin

Polyols

Polyols have the advantageous characteristic of a reduced volume alteration. The primary drawbacks are elevated phase transition temperatures, less latent heat, and substantial costs [123].

III. Eutectics

They are combinations of organic-organic, organic-inorganic, and inorganic-inorganic mixes. The important point in eutectics is that the melting temperatures of the components must be the same; therefore, eutectics behave as pure materials [125].

2.6.2. Researches for enhancement methods the adding PCM in the refrigeration system

PCMs are becoming increasingly popular in refrigeration systems due to their ability to increase efficiency, reduce energy consumption, and improve temperature stability.

Chapter 3

Study regarding the use of PCMs for the defrost of VCRs considering multiple refrigerants

In this chapter, another source of heat obtained by recovering the thermal energy available in the gases discharged by the compressor during the operation of the VCRs is fundamentally proposed and theoretically analysed. From here it follows a new defrosting method that uses this recovered thermal energy. To use this thermal energy, it is necessary to store it so that it can be used during the defrosting period, a storage option is the PCM phase change materials. This chapter investigates the effectiveness of adding Phase Change Materials (PCMs) to refrigeration systems, a mathematical model has been proposed. The model was applied in the first stage for R404a freon, using experimental determinations made on an existing installation in a famous fast-food chain. The model analyzes the performance of using PCMs in defrosting Vapor Compression Refrigeration (VCR) systems with various refrigerants including R600a, R600, R1234yf, R404a, R134a, R1234ze(e) and R152a and another refrigerant listed in document R600. The goal of this model is to assess the performance of the RS with the addition of PCMs.

3.1 Mode of operation of VCRs by Incorporating Phase Change Materials

This method involves the introduction of a recuperative heat exchanger with thermal energy storage function between the compressor and the condenser. This functional component can recover and store thermal energy, using PCMs, from the refrigerant discharged by the compressor. During this process the phase change materials (PCMs) melts. Phase change heat storage materials are stocked in the recuperative heat exchanger, PCMhx, as seen in Figure 3.1.

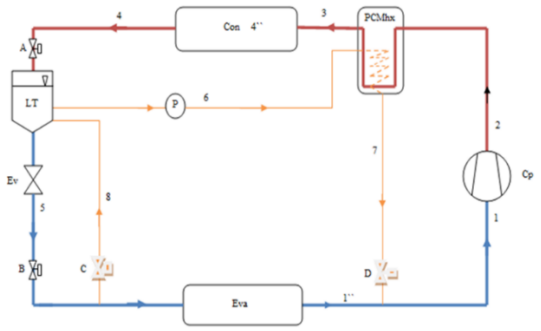


Figure 3.1 Schematic view of the refrigeration system

3.2 Refrigeration Cycle on a p-h Diagram of VCRs by Incorporating Phase Change Materials

The Refrigeration Cycle and defrosting process of VCRs with PCM are presented in Figure 3.2 in a p-h Diagram. Where states 1", 1, 2, 3, 4 and 5 are characteristic of the RS operating cycle and the states 6, 7, 8 are characteristic of the PCM defrost cycle.

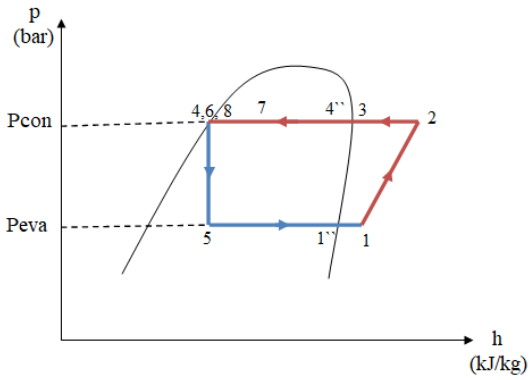


Figure 3.2 Thermodynamic cycle of the VCRs with PCM

Using the first law of thermodynamics it is calculated the specific thermal load by the recuperative heat exchanger:

$$q_{3-2} = h_3 - h_2 \quad (3.1)$$

Using the first law of thermodynamics the specific heat flux is calculated by the recuperative heat exchanger:

$$q_{6-7} = h_7 - h_6 \quad (3.2)$$

It calculates the specific input work at pump:

$$w_{8-6} = v(p_6 - p_8) \quad (3.3)$$

3.3 Modelling of the PCMs defrost refrigeration system

The operating conditions for which the mathematical model was applied are the following: t_o =-30°C, t_c =33°C, Δt_{sh}=15°C, m_{ice} =1.4 kg, Δp =0.6 bar, $\dot{Q}_o$ =4.5kW, R404A

The heat flux transfer from the heat exchanger PCMs

$$\dot{Q}_{pcmhx} = \dot{m}_{ref} \cdot q_{pcmhx} \quad (3.4)$$

$Q_{recovery}$ is the maximum storage by PCM

$$Q_{recovery} = \dot{Q}_{pcmhx} \cdot \tau_{cooling} \quad (3.5)$$

$\dot{Q}_{defrost}$ is the heat flux transfer from the refrigerant in the defrost process

$$\dot{Q}_{defrost} = \dot{m}_{defrost} \cdot (h_7 - h_6) \quad (3.6)$$

Q_{ice} is the heat received by ice in the defrost process

$$Q_{ice} = m_{ice} \cdot [c_{ice} \cdot (0 - t_{ice}) + \lambda_{ice}] + m_{drain_w} \cdot c_w \cdot (t_{w2} - 0) \quad (3.7)$$

$\dot{Q}_{defrost}$ is the heat flux transfer in defrosting process discharged by PCM

$$\dot{Q}_{defrost} = m_{pcm} \cdot \frac{\lambda_{pcm}}{\tau_{soldification}} \quad (3.8)$$

P_{p_1} the pump power consumption

$$P_{p_1} = \dot{m}_{ref} \cdot w_{8-6} \quad (3.9)$$

The coefficient of performance COP including the defrosting process with PCM

$$COP_{with\ pump} = \frac{\dot{Q}_0}{P + P_{p_1}} \quad (3.10)$$

3.4. Results and Discussions

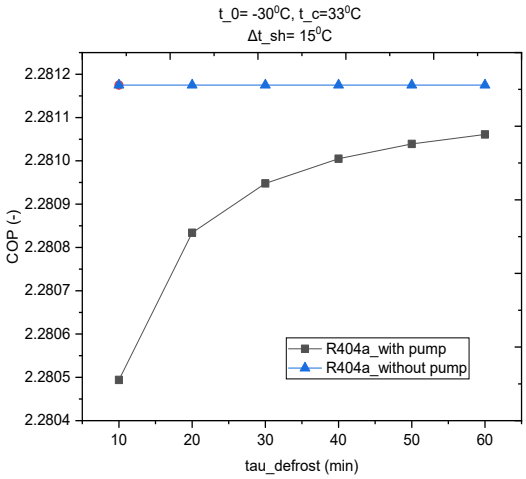


Figure 3.3 - Comparison between COP with pump and COP without pump

The coefficient of performance (COP) increases slowly with the increase of the defrosting time. It can be seen that the $COP_{with\ pump}$ of the refrigeration system with a PCM based defrosting is lower than the case of the refrigeration system without (PCM). This is due to the fact that the power of the pump has a low value which means that for both situations the coefficient of performance shows very close in values.

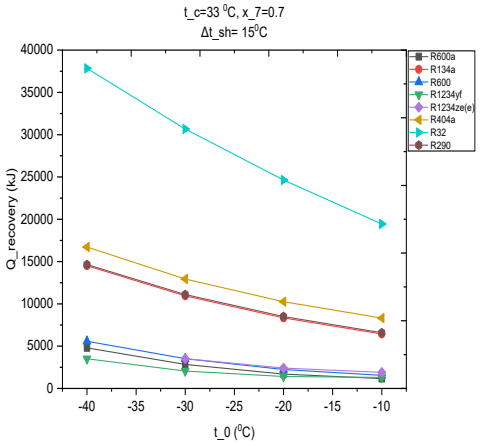


Figure 3.4 – Variation of evaporation temperature with PCM heat recovery

The figure shows that increasing the evaporating temperature leads to a decrease of the recovered heat. Also, one can notice the heat recovered in the case when the refrigeration system operates at freezing temperatures (-15°C to -40°C) is higher compared to the case when it operates at refrigeration temperatures (-10°C to -15°C). This happens because when the evaporating temperature decreases the evaporating pressure decreases also which means higher compression ratio and as a result higher compressor discharge temperature t_2.

Figure 3.5 shows that the increase of the condensing temperature t_c leads to an increase in the heat recovery

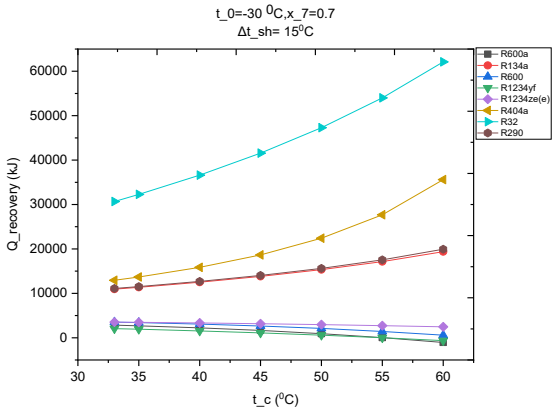


Figure 3.5 - Variation of condensing temperature with PCM heat recovery

Chapter 4

Experimental Analysis of Air or Electric Heater Defrosting in a VCRS

The experimental research was conducted on two setups with two main objectives:

1. To establish the operating conditions of a VCRS capable of maintaining a temperature of 1–4 °C in a small refrigeration chamber.
2. To determine the thermophysical properties of a PCM suitable for storing thermal energy from the discharge gases of a VCRS compressor, which can be used for defrosting.

4.1 Experimental rig

Figure 4.1 presents a schematic representation of the experimental setup of the VCRS used in this study.

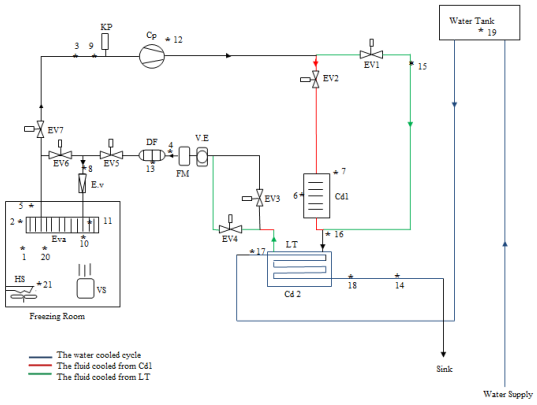


Figure 4.1 Schematic of the installation of the VCRS

➢ **The refrigeration loop**

The refrigeration loop which consists of: Compressor (Cp), condenser (Cd), and evaporator

4.1.1. Evaporator (Eva)

The Eva is a heat exchanger that transfers heat from the space of the refrigerator compartment through its walls or the tubes used in its construction to the refrigerant inside it.

4.1.2. Compressor (Cp)

A Cp is a mechanical device used to elevate the pressure and temperature of the refrigerant transitioning from the Eva, characterized by low pressure, to the Con, characterized by high pressure.

4.1.3. Condenser (Cd)

The Con is used to remove heat from the fluid (refrigerant) and discharge it into the environment.

- **Drier filter and sight glass**

The filter drier serves an important role in each refrigeration system, its function is to retain the moisture content and impurities from the refrigerant caused by the operation of the VCRS, which prevents the refrigerant flow channel through the E.v from being blocked. The function of the sight glass is to detect the presence of liquid refrigerant and moisture content.

4.1.4. Expansion valve (E.v)

The E.v is a device that is used to reduce the high pressure in the Con to the low pressure in the Eva

- **pipes and thermal insulation**

The RS consists of connection pipes that link several components. These connection pipes are constructed using copper material

- **Measuring devices used in the experimental stand VCRs**
- **Temperature measurement**

two temperature sensors used in the experimental setup. Tow kind of temperature sensors used, the NTC contact and notice the non-contact air NTC sensor that is used for measuring air temperature inside the cold room.

- **Pressure measurement**

Two pressure sensors are used. For measuring the suction pressure and for measuring the condensing pressure

- **Control panel**

the control panel with the Dixell controllers used to read the temperature, pressure and humidity values at the selected positions on the experimental loop.

- **Data acquisition device**

the measured quantities on the VCRS experimental stand recorded, storage and transmission using a special device (XWEB500-EVO)

- **The heat source**

To ensure the uninterrupted functionality of the VCRS experimental stand and simulate a thermal load, a heat source was placed inside the refrigerated room

- **Variable voltage power source device**

The regulation of the air heater's functioning is achieved using a DIXELL XR20CX temperature regulator. The temperature regulator is installed inside a housing that is situated within the cold room.

- **The operation of the experimental stand**

The operation of the stand using the Cd1 requires the opening of the electromagnetic valves EV1, EV4, EV5, EV6 and EV7 (Figure 4.1), respectively the closing of EV2 and EV3.

4.2 Results and discussion

This section presents the results of the experimental study. It contains a comparative analysis over functional parameters of the VCRS using electric heating defrosting and Air defrosting. . From this experimental analysis, several determinations were extracted, carried out under the following conditions (see Table 4.1).

Table 4.1 Physical and Thermal Conditions under which the Experimental Determinations were Carried Out

	Electric defrosting	Air defrosting
Ambient temperature	25°C	25°C
Ambient relative humidity	65%	30%
Ambient moisture content	$6 \cdot 10^{-3} kg_v/kg_{aus}$	$6 \cdot 10^{-3} kg_v/kg_{aus}$
Temperature inside the cooled space	4°C	4°C

Figures 4.2a and **4.2b** show the variation in instantaneous power consumption by the compressor throughout a complete operating cycle for both defrosting methods. In area Ia, the power consumed by the compressor is lower in variant a (electric defrosting) than in variant b (air defrosting) until the system reaches a stable operating condition. However, the average power consumed by the compressor in both situations is approximately the same, 484 W for electric defrosting and 482 W for air defrosting.

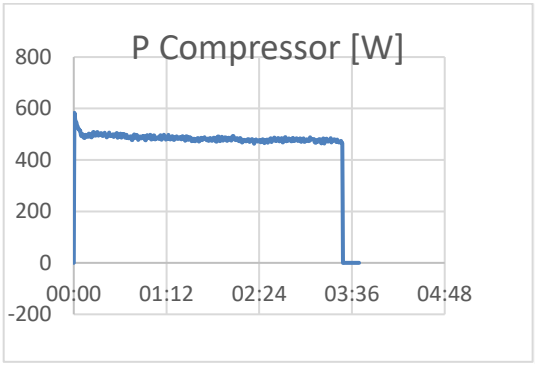


Figure 4.2a Variation of power at compressor in time (Electric Heating defrosting)

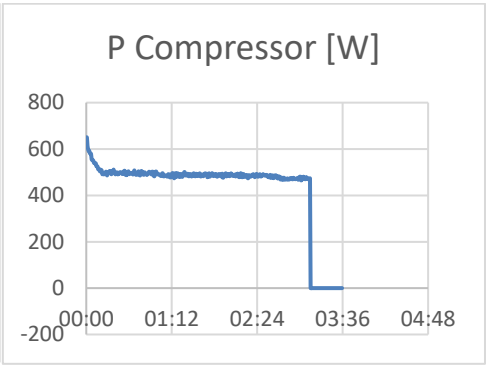


Figure 4.2b Variation of power at compressor in time (Air defrosting)

Figures 4.3a and **4.3b** present how the electrical power required for the defrosting process changes over time. As anticipated, the instantaneous power consumed in variant (a) is greater than in variant (b). However, the duration of the defrosting process is also important, as it affects both the average and total energy consumption.

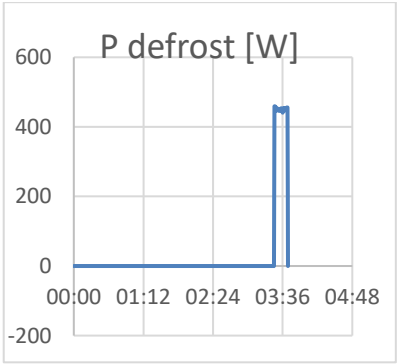


Figure 4.3a Variation of defrost power in time (Electric Heating defrosting)

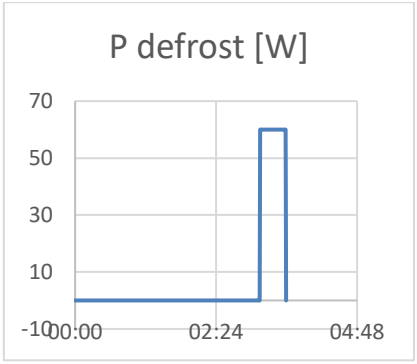


Figure 4.3b Variation of defrost power in time (Air defrosting)

Figures 4.4a and **4.4b** show the total energy consumption of two systems over time. It is observed that the system utilizing electric defrosting consumes more energy than the one using air defrosting. Specifically, the energy consumption for the electric defrosting system is 2.6 kWh, compared to 2.4 kWh for the air defrosting system, resulting in a difference of approximately 8%. This discrepancy can be attributed to the electric resistance, which consumes about seven times more energy than the fan. Although the electric resistance operates for half the time of the fan during the defrosting period, the total energy consumption throughout an entire refrigeration-defrosting cycle remains higher for the electric defrosting system than for the air defrosting system.

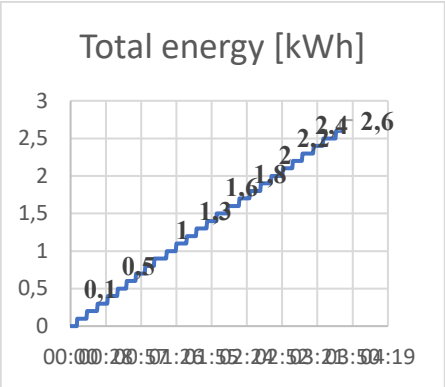


Figure 4.4a Variation of total energy in time (Electric Heating defrosting)

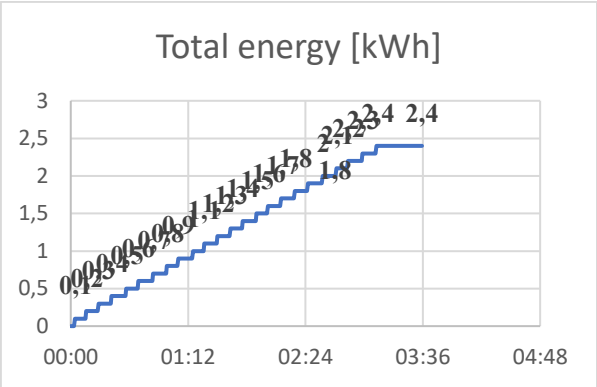


Figure 4.4b Variation of total energy in time (Air defrosting)

Chapter 5
Experimental Study of PCM for Thermal Energy Storage

This chapter focuses on the second experimental objective, which consists of determining the latent heat of fusion of a specific PCM, as well as the functional analysis of a tube-in-tube thermal energy storage unit using this PCM.

5.1 Experimental rig

The experimental configuration was designed to investigate the effects of inlet temperature and flow rate fluctuations on the performance of the melting and solidification processes of the PCM inside vertical shell and tube heat exchanger (VSTHX) systems. Figures 5.2 and 5.1 show the schematic and photograph of the experimental loop.

5.1.1 Test section

This experimental investigation used a vertical configuration for the shell and tube heat exchanger, the test section included the shell, tube, upper plastic cover, and PCM.

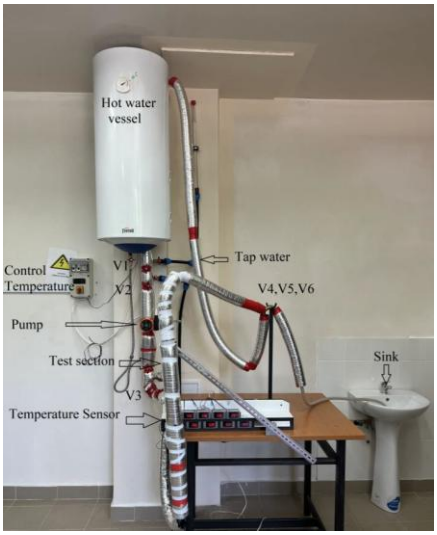


Figure 5.1 The components of the experimental rig

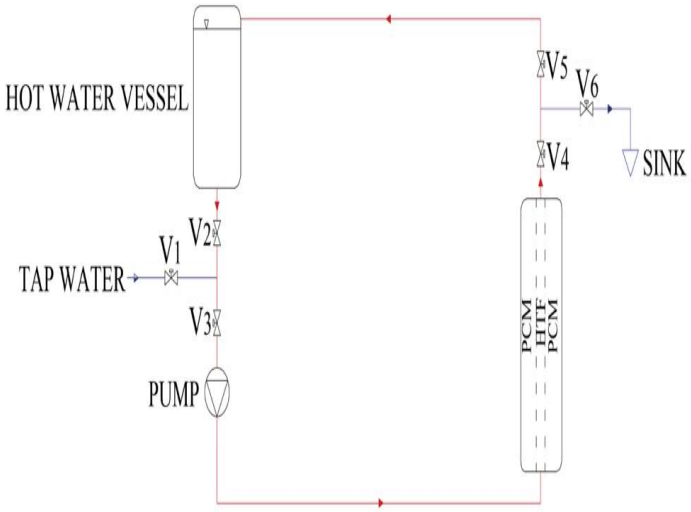


Figure 5.2 Schematic diagram of the experimental Loop

- **Shell**

Is a copper tube with a length of 1 meter, an outside diameter of 28 millimeters and a shell thickness of about 1 millimeter.

- **Tube**

copper tube of 1.2 m in length, with an external diameter of 10 mm and a thickness of around 1 mm.

- **Cap**

A plastic cap was used to seal the top end of the tube, to prevent any possible leakage of liquid phase change material (PCM) during the melting process.

- **Phase change materials (PCM)**
  Five types of PCMs were utilized as thermal energy storage in the present work: RT 54 HC, RT 44 HC, RT 35 HC, SP 50, and SP 31 (Rubitherm).

5.1.2 Auxiliary equipment

The main purpose of the test tube is to store the thermal energy accumulated in the thermal energy storage (TES) system, represented by PCM. The stored energy is transferred by a heat transfer fluid (HTF), represented by water, which circulates in a closed loop through the test section.

5.1.2.1 Hot water vessel

Hot water vessel used in the experimental rig is an electrical boiler. The electric heater functions as a source of thermal energy by converting electrical energy into heat.

- **Charging process (melting process)**

The hot water flow required for the PCM melting process is provided by the boiler described previously. The hot water (HTF) was produced at temperatures higher than the melting temperature of the tested PCM. For the SP50 PCM, the tests were conducted with water at 60, 65, and 70 °C, ensuring a melting temperature difference of approximately 5, 10, and 15 °C. The tests were carried out for different water flow rates in the range of 0.009–0.020 kg/s. In the SP50 tests, the hot water flow rate for heating was 0.097 kg/s for a water temperature of 60 °C. In this case, valves V2, V3, V4, and V5 are open, while V1 and V6 are closed. The flow rate is adjusted using valves V2 and V3.

- **Discharging process (solidification process)**

Cold water is used in an open-loop system, supplied by the municipal source. During the discharge (PCM solidification) phase, valves V1, V3, V4, and V6 are open, while V2 and V5 are closed.

- **Phase change materials**

In this study, five different types of commercial paraffin, which are RT 54 HC, RT 44 HC, RT 35 HC, SP 50, and SP 31 (Rubitherm), were utilized as PCM. Experimental investigations were conducted on these paraffin types to determine the onset and completion points of melting and solidification, as well as the corresponding latent heat values. The obtained experimental data were subsequently employed in the theoretical analysis [171] to assess the amount of heat that could be effectively recovered and stored for the defrosting process of the VCRS, considering the following refrigerants: R600a, R600, R1234yf, R1234ze, R152a, R290, and R32.

5.1.3 Measurement Devices

In conducting the experimental study, equipment was used for temperature measurement (contact sensors and immersion sensors), a hot water flow meter, and digital controllers for signal acquisition and processing.

5.1.3.1 Temperature sensor

To monitor the processes occurring in the PCM, the VSTHX was equipped with nine temperature sensors, as shown in Figure 5.3. In this way, the PCM temperature was monitored at five levels (see Table 5.1), corresponding to points 1, 2, 3, 4, and 5. The significance of the temperature sensors mounted along the VSTHX is presented in Table 5.1. Sensors T1 and T2 measure the water temperature at the inlet and outlet of the tube. Sensors T4, T5, T6, and T7 measure the temperature at the five levels on the outer surface of the VSTHX, while sensors T8 and T9 measure the PCM temperature in the inter-tubular space.

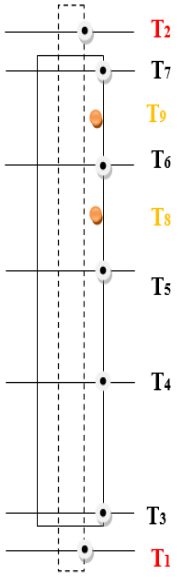


Figure 5.3 Temperature sensor placement on the VSTHX

Table 5.1. Temperature sensors on the VSTHX

VSTHX level	Measurement points	Measurement point description
	T_1	Inlet hot/cold water temperature
	T_2	Outlet hot/cold water temperature
1	T_3	Temperature at level 1 on the surface of the VSTHX
2	T_4	Temperature at level 2 on the surface of the VSTHX
3	T_5	Temperature at level 3 on the surface of the VSTHX
4	T_6	Temperature at level 4 on the surface of the VSTHX
5	T_7	Temperature at level 5 on the surface of the VSTHX
	T_8	Temperature of the PCM between levels 3 and 4
	T_9	Temperature of the PCM between levels 4 and 5

5.1.3.2 Flow meter water

The flow rate of hot water during the melting cycle, as well as the flow rate of cold water during the solidification cycle, is measured using a flow meter.

5.1.3.3 Stopwatch

The timing basis for conducting the experimental measurements was provided by the EMERSON console and the computer used for data downloading.

5.2. Results and discussion

This chapter presents experimental data obtained for the SP50 PCM. Figure 5.4 shows the variation of the PCM temperature. The graph shows two average temperatures. The total average temperature represents the average of all temperatures characterizing the PCM on all seven levels. The average external temperature represents the average between the five temperatures measured on the outside of the tube. From the graph, seven zones are identified that characterize a complete cycle of heating, melting, overheating, thermal equilibrium, desuperheating, solidification,

subcooling and thermal equilibrium**.** The difference between the two average temperatures can be explained by the fact that the temperature measured by sensors immersed in the PCM raises the value of the average temperature. Evaluating the temperature with sensors mounted on the outside of the tube introduces an error due to the thermal resistance of the wall, resulting in a temperature difference between the PCM and the exterior of the tube.

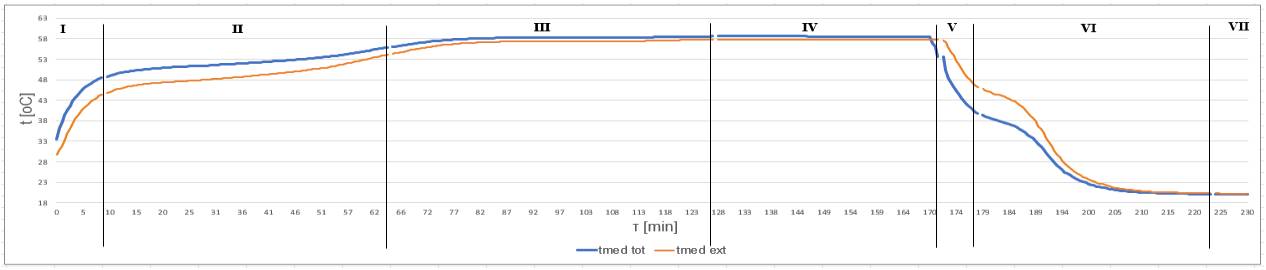


Figure 5.4 Evolution of the average PCM temperature in time

In Figure 5.5, the variation of the water temperature at the inlet and outlet of the VSTHX is presented. The temperature difference can be observed, which is initially large approximately 20 °C until the component parts reach thermal equilibrium, after which it decreases significantly. In the thermal equilibrium zone IV, it stabilizes at 1 °C.

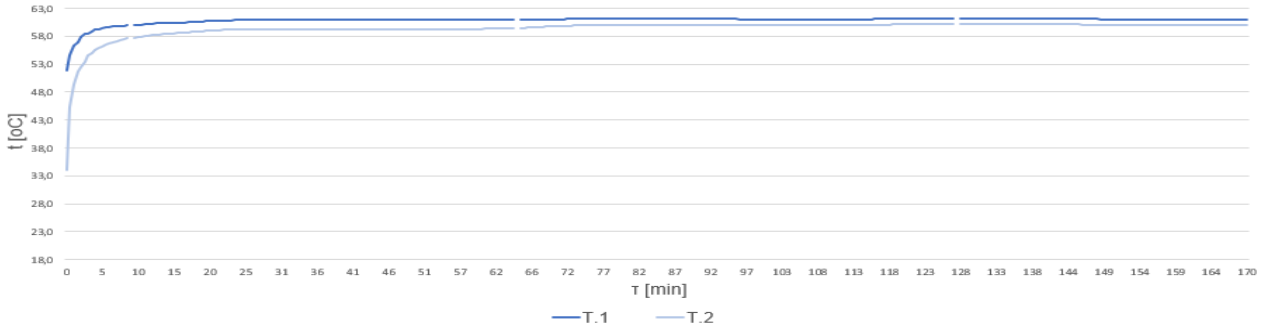


Figure 5.5 Water temperature variation at the inlet and outlet during the PCM melting process

Figure 5.6 is relevant because it shows that the melting process, as well as the solidification process, does not occur continuously across all sections of the tube. This means that at the lower levels, melting does not progress uniformly along the height of the tube. There are lower zones where the PCM remains solid, while in the upper zones, melting has already begun. This can be explained by two hypotheses: rapid conduction at the outer tube level, and the upward movement of the melted and superheated PCM toward the upper sections of the tube, which promotes the initiation of paraffin melting.

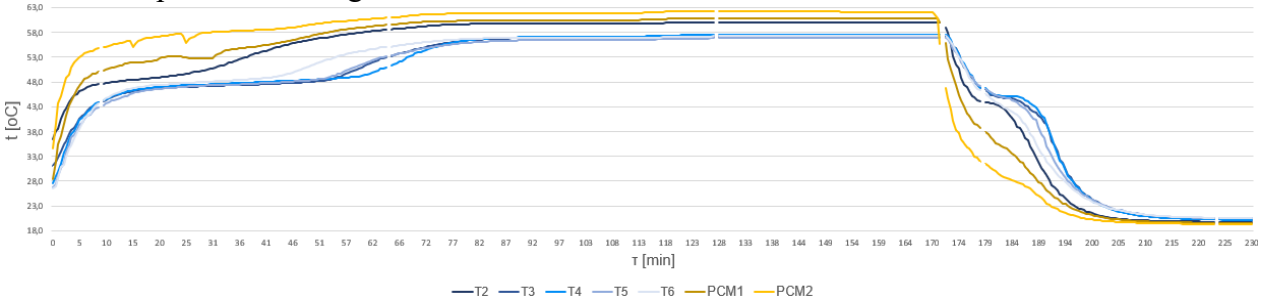


Figure 5.6 Temperature variation of SP50 along the tube across the seven analyzed sections

From the heat balance equation, an average latent heat of melting and solidification is calculated for the entire process

$$Q_{PCM} = \left(\dot{Q}_w - \dot{Q}_{amb}\right) \cdot \tau_{process} - Q_{cooper} \quad 5.1$$

The heat flow delivered by the hot water:

$$\dot{Q}_W = \dot{m}_w \cdot \bar{c}_w \cdot \overline{\Delta t}_w \quad 5.2$$

The heat flow delivered by the hot water

$$\dot{Q}_{amb} = \dot{m}_w \cdot \bar{c}_w \cdot \overline{\Delta t}_{weq} \quad 5.3$$

The heat absorbed by the tube and the copper components

$$Q_{cooper} = m_{cooper} \cdot c_{cooper} \cdot \Delta t_{cooper} \quad 5.4$$

As stated at the beginning of the chapter, the experimental determinations performed provide interesting information regarding the way in which the phase change occurs vertically in the tube. The average temperature provides important information in this regard. For a water temperature of 60°C, figure 5.7 shows the evolution of the melting process of SP50 in the 5 sections where sensors are mounted on the outside of the tube. The orange area represents the melting range of the PCM (50-51°C) performed in the five measurement sections. It is observed that the melting temperature is reached first in the base section, section 1, then "surprisingly" the next section where melting occurs is on level 5, at the top of the tube. Melting continues level 2 towards the base then on level 4 towards the end of the tube. The section where melting occurs at the latest is section 3 in the middle of the tube. The process is not surprising if we take into account the two hypotheses mentioned earlier: a high rate of heat transfer by conduction along the outer tube, and an upward gravitational movement of the melted and superheated paraffin, which promotes the melting of paraffin in the upper sections 4 and 5.

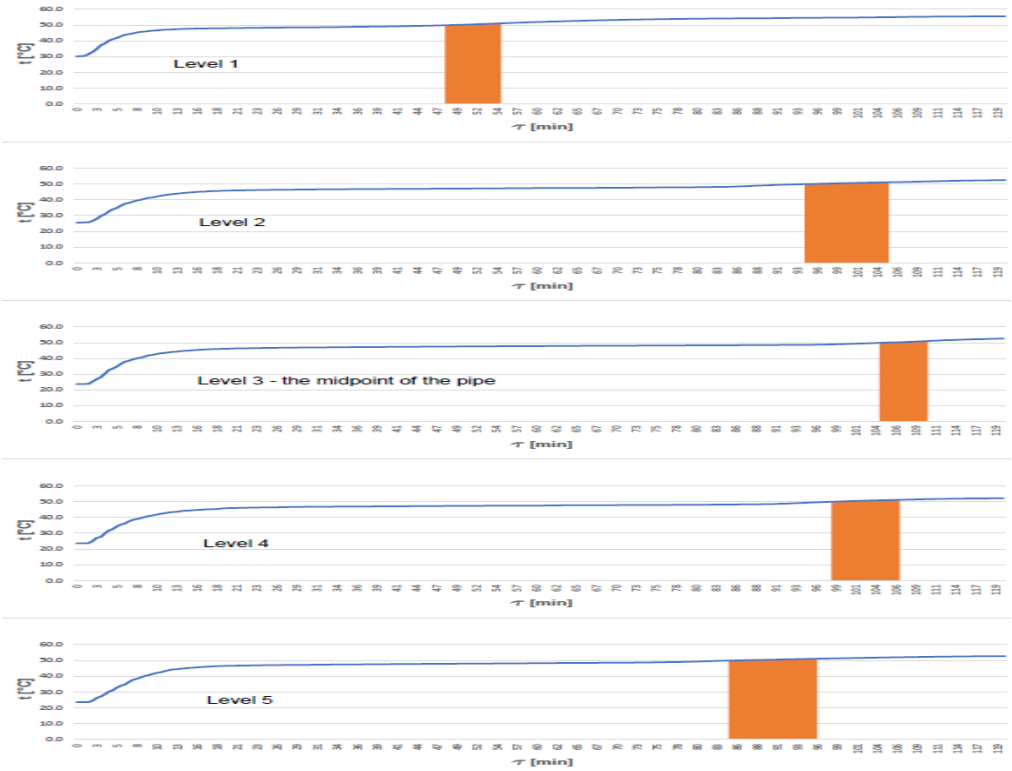


Figure 5.7. Analysis of temperature profiles along the pipe during PCM phase change at a water temperature of 60 °C

Using a water flow rate of 65 °C accelerates the melting process of the paraffin. This aspect is shown in figure 5.8. In the base section, the melting is initiated after 26 minutes compared to 48

minutes when using a water flow of 60ºC. The melting is also completed in the median section after 64 minutes compared to 110 minutes when using a water flow of 60ºC.

Figure 5.9 shows the evolution of SP50 melting in the case of VSTHX being supplied with 70ºC water. As in the previous case, increasing the water temperature shortens the melting time. Melting starts in the base section after 20 minutes. The finish is also in the median section 3 and is done after 42 minutes.

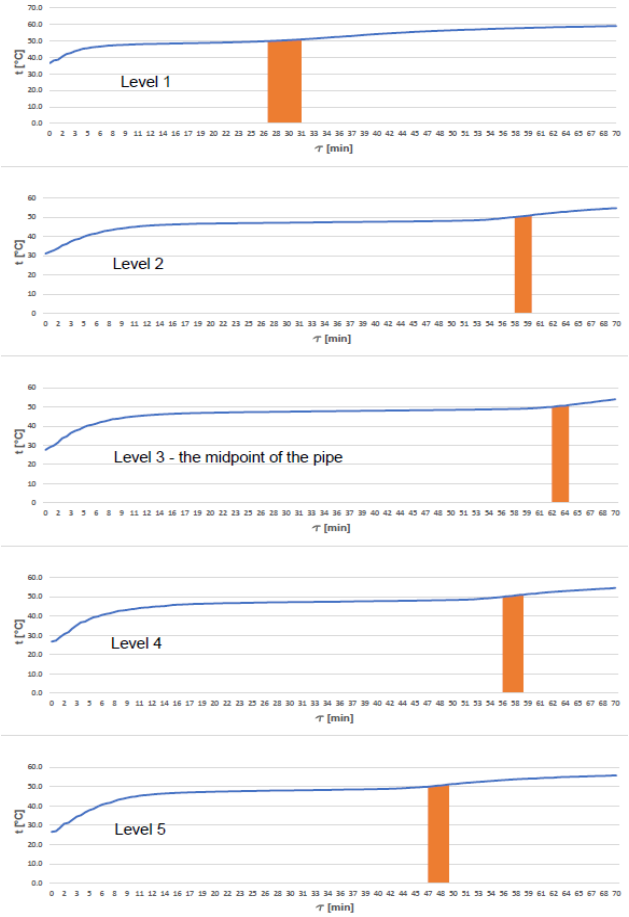


Figure 5.8 Analysis of temperature profiles along the pipe during PCM phase change at a water temperature of 65 °C

As a synthesis of the results presented in Figures 5.6, 5.7, and 5.8, Figure 5.9 shows the impact of water temperature on the phase-change interval of PCM SP50.

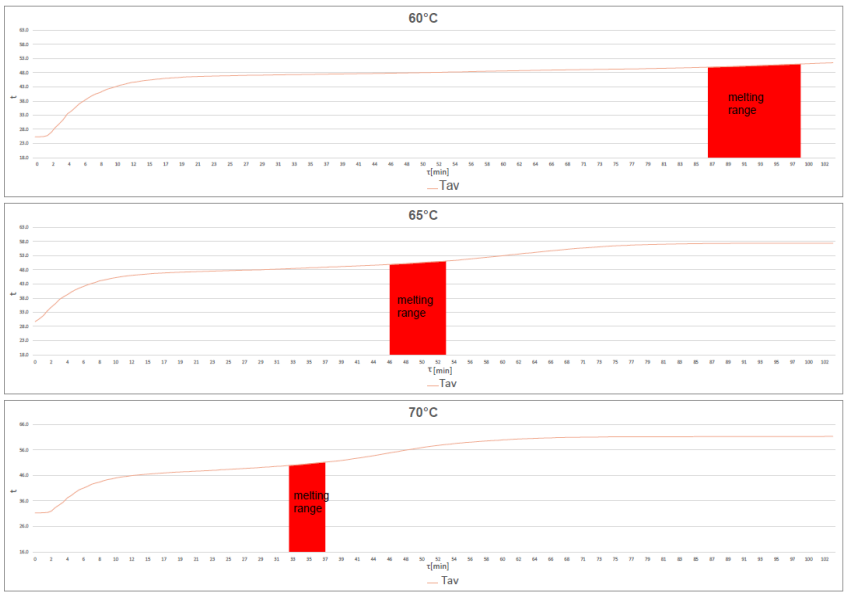


Figure 5.9 Impact of water temperature on the PCM- SP50 phase-change interval

It is observed that as the water temperature increases, the initiation and completion of the melting process is faster, and the melting interval is shorter. These conclusions can be drawn from the analysis of how the average temperature in the tube evolves over time. The melting start and end intervals are defined by the temperatures of 50 and 51°C respectively.

Chapter 6
Comparison between defrosting methods using different refrigerants

In this chapter, the performance analysis of a refrigeration system operating with different refrigerants was conducted for four defrosting methods (air, electric heating, hot gas and PCM) within an existing refrigeration system in the laboratory of Engineering Thermodynamics, Department of Thermodynamics, Engines, Thermal and Refrigeration Equipment, Faculty of Mechanical and Mechatronic Engineering, National University of Science and Technology POLITEHNICA Bucharest, Romania. Thermodynamic analyses were conducted on refrigerants: R290, R134a, R600a, R600, R404A, R32, R1234yf, and R1234ze(E) over a 24-hour period for refrigeration.

6.1. Introduction

The defrosting method involves storing thermal energy from the compressor discharge gases by using a Phase Change Material (PCM). It can be applied to VCR systems under certain operating conditions and for specific refrigerants (as presented in this chapter). The advantages of this system combine the benefits of hot gas defrosting with reduced energy consumption and the protection of the evaporator, as the temperature of the defrosting medium is lower than in the case of hot gas defrosting.

6.2. The mathematical model of a VCRS with defrosting process

In this paragraph, the effects of different defrosting methods (air, electric heating, hot gas and PCM) for solving the frost issue were investigated theoretically [167]. The approach is carried out in two stages:

- from the following list of refrigerants: R134a, R32, R404A, R1234yf, R1234ze(E), R600, R600a, R290 those are selected which, from a theoretical standpoint, meet the condition for storing thermal energy sufficient to enable PCM-based defrosting (discharge temperature and the recoverable and storable thermal energy);

- for the selected refrigerants, a comparative study is carried out regarding energy efficiency (COP) for four defrosting methods: air defrosting, electrical defrosting, hot gas defrosting, and PCM-based defrosting. Since it is the same system, the operation of the VCRS during the cooling operating mode is identical, whereas the operation during the defrosting operating mode differs. As a result, the mathematical model for the cooling mode is the same, but it is different for the defrosting period.

The operating cycle of the VCRS during the cooling operating mode for the four defrosting methods is shown in Figure 6.1, where:

1–2: compression process,2–3: desuperheating,3–4: condensation and subcooling, 4–5: throttling,5–1": evaporation, 1"–1: superheating.

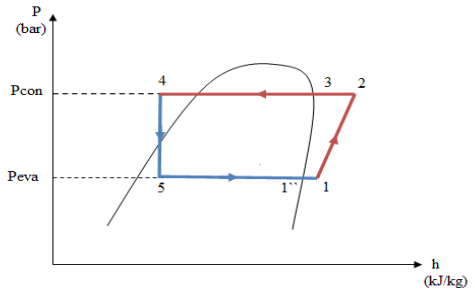


Figure 6.1. Thermodynamic cycle of VCRs with PCM

Figures 6.2, 6.3, 6.4, and 6.5 show the operating schematics of the VCRS with the four defrosting systems, where Eva is the evaporator, Cp the compressor, Con the condenser, E.v the throttling valve, F_1 the evaporator fan, F_2 the condenser fan, LR the liquid receiver/liquid tank, EH the electric heater, CT the capillary tube, P the pump, LS the liquid separator, and PCMhx the PCM heat exchanger.

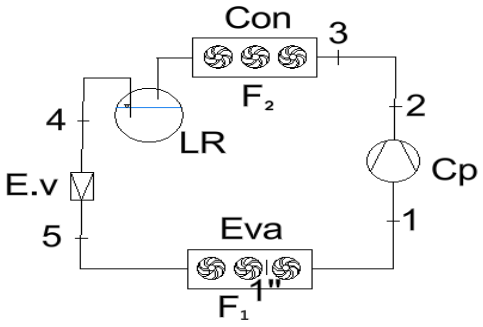


Figure. 6.2. Air defrost method

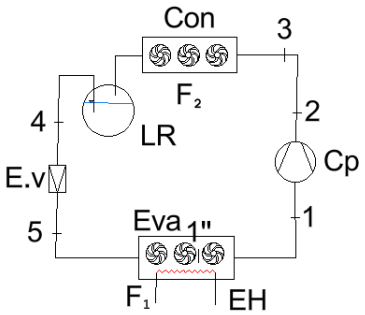


Figure 6.3. Electric heating defrost method

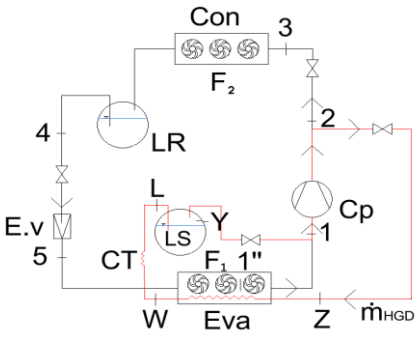


Figure. 6.4. Hot gas defrost method

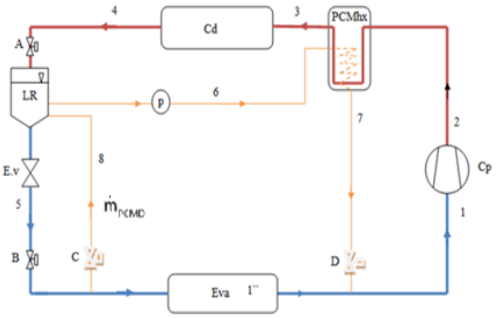


Figure. 6.5. PCM defrost method

The equipment was used to analyze the four types of defrosting considering the following refrigerants: R290, R134a, R600a, R600, R404A, R32, R1234yf, and R1234ze(E). The analysis was conducted utilizing the Engineering Equation Solver software [168]. The mathematical model was constructed based on scientific articles [164,167, 169,170].

6.2.1 The mathematical model for VCRS air defrosting

The total electric power demand $\dot{E}_{cons}$, as expressed in Equations (6.1) was calculated for air defrosting:

$$\dot{E}_{cons} = z_{24h}^{cycle} \cdot \left[\frac{\tau_{cooling}}{\tau_{cycle}} \cdot (P_{cp} + P_{F_1} + P_{F_2}) + \frac{\tau_{defrost}}{\tau_{cycle}} \cdot P_{F_1} \right] \quad 6.1$$

The coefficient of performance (COP) of the refrigeration cycle with and without defrosting are [167]:

$$COP_c = \frac{\dot{Q}_0}{P_{cp}} \quad [-] \quad 6.2$$

$$COP_{with\,defrost} = \frac{\dot{Q}_0}{\dot{E}_{cons}} \quad [-] \quad 6.3$$

The mathematical model was built based on the flow chart shown in Figure 6.6.

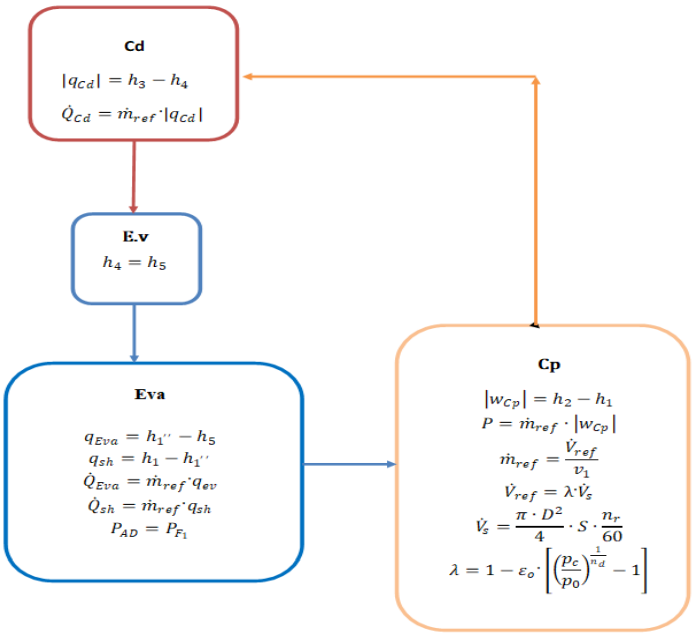


Figure 6.6. Flowchart of mathematical modeling for VCRS with Air defrost

6.2.2 The mathematical model for VCRS electric heater defrosting

The total electric power demand $\dot{E}_{cons}$, as expressed in Equations (6.4)

$$\dot{E}_{cons} = z_{24h}^{cycle} \cdot \left[\frac{\tau_{cooling}}{\tau_{cycle}} \cdot (P_{cp} + P_{F_1} + P_{F_2}) + \frac{\tau_{defrost}}{\tau_{cycle}} \cdot P_{EHD} \right] \quad 6.4$$

The coefficient of performance (COP) of the refrigeration cycle with and without defrosting are [167]:

$$COP_c = \frac{\dot{Q}_0}{P_{cp}} \quad [-] \quad 6.5$$

$$COP_{with\,defrost} = \frac{\dot{Q}_0}{\dot{E}_{cons}} \quad [-] \quad 6.6$$

The mathematical model was built based on the flow chart shown in Figure 6.7.

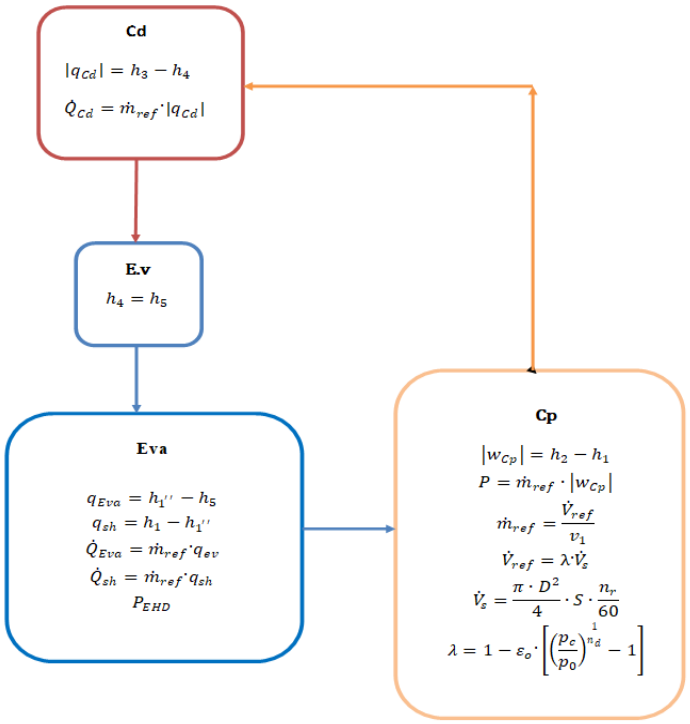


Figure 6.7. Flowchart of mathematical modeling for VCRS with Electric Heater Defrost

6.2.3 The mathematical model for VCRS hot gas defrosting

The total electric power demand $\dot{E}_{cons}$, as expressed in Equations (6.7) was calculated for air defrosting:

$$\dot{E}_{cons} = z_{24h}^{cycle} \cdot \left[\frac{\tau_{cooling}}{\tau_{cycle}} \cdot (P_{cp} + P_{F_1} + P_{F_2}) + \frac{\tau_{defrost}}{\tau_{cycle}} \cdot P_{HGD} \right] \quad 6.7$$

The coefficient of performance (COP) of the refrigeration cycle with and without defrosting are [167]:

$$COP_c = \frac{\dot{Q}_0}{P_{cp}} \quad [-] \quad 6.8$$

$$COP_{with\,defrost} = \frac{\dot{Q}_0}{\dot{E}_{cons}} \quad [-] \quad 6.9$$

The mathematical model was built based on the flow chart shown in Figure 6.8.

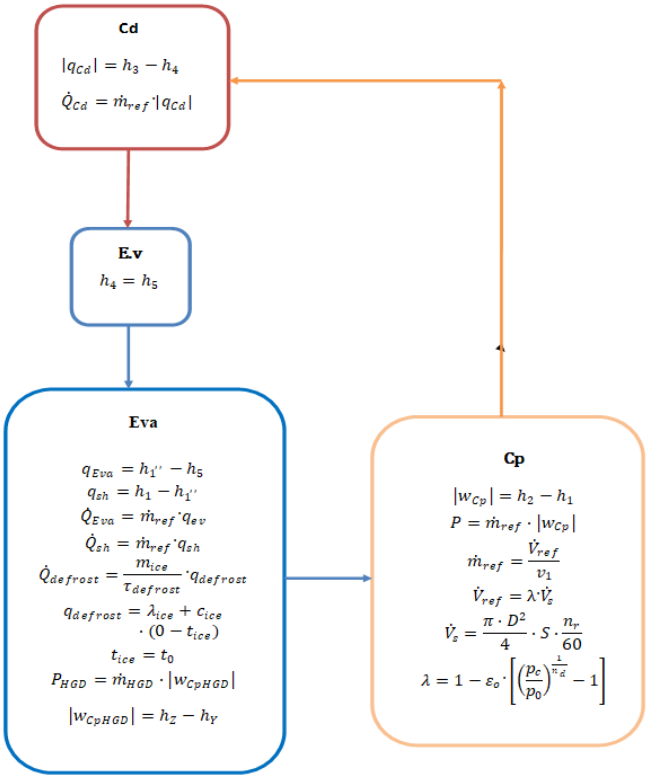


Figure 6.8. Flowchart of mathematical modeling for VCRS with Hot Gas Defrost

6.2.4 The mathematical model for VCRS PCM defrosting

The total electric power demand $\dot{E}_{cons}$, as expressed in Equations (6.10) was calculated for air defrosting:

$$\dot{E}_{cons} = z_{24h}^{cycle} \cdot \left[\frac{\tau_{cooling}}{\tau_{cycle}} \cdot (P_{cp} + P_{F_1} + P_{F_2}) + \frac{\tau_{defrost}}{\tau_{cycle}} \cdot P_{PCM\,D} \right] \quad 6.10$$

The coefficient of performance (COP) of the refrigeration cycle with and without defrosting are [167]:

$$COP_c = \frac{\dot{Q}_0}{P_{cp}} \quad [-] \quad 6.11$$

$$COP_{with\,defrost} = \frac{\dot{Q}_0}{\dot{E}_{cons}} \quad [-] \quad 6.12$$

The mathematical model was built based on the flow chart shown in Figure 6.9.

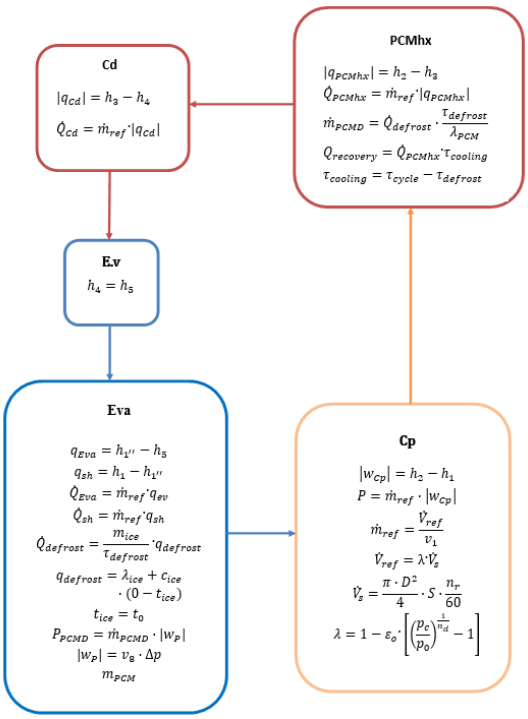


Figure 6.9. Flowchart of mathematical modeling for VCRS with PCM Defrost

6.3. Results and discussion

In the first stage, the capacity to recover thermal energy from the discharge gases for PCM defrosting was evaluated through two parameters: discharge temperature and the amount of heat that can be recovered and stored. Based on the thermophysical properties specific to PCM SP50, a selection was made of the refrigerants for which the use of this substance for PCM defrosting is feasible.

In the second stage, the mathematical models were run for all types of defrosting (air, electric heater, hot gas, and PCM), carrying out a comparative analysis of the VCRS operation over a 24-hour period for the selected refrigerants. The mathematical models for all the selected refrigerants were run based on experimentally determined temperatures, considering isentropic compression. For the "R404 exp" regime, the specific consumption and the compressor power were determined based on the discharge temperature measured on the installation.

Figure 6.10 presents, in a centralized manner, the compressor discharge temperatures obtained from the calculations for all the analyzed refrigerants. It can be observed that only some of them are characterized by a temperature higher than the melting temperature of the PCM SP50 ($t_{melting}$ = 50–51 °C).

The discharge temperature level of the other refrigerants (see Figure 6.10) and the Δh from the desuperheating process which determines the storable thermal energy (see Figure 6.11) do not allow heat recovery from the compression process during the cooling operating mode; therefore, the analysis was performed only for the refrigerants R290, R404A, R32, and R134a.

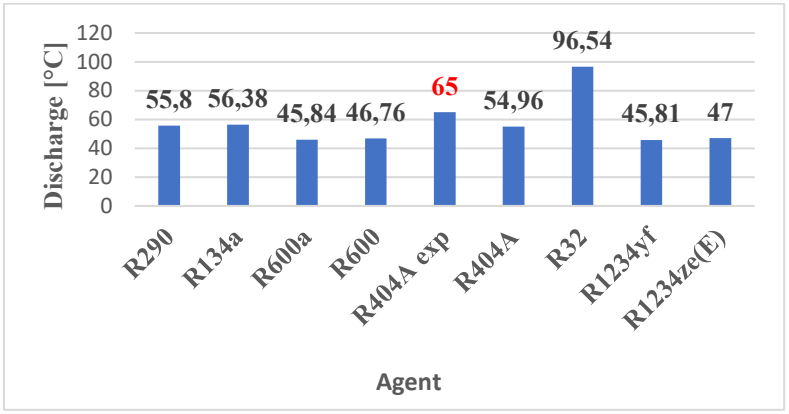


Figure 6.10. shows the discharge temperature from the compressor for all refrigerants.

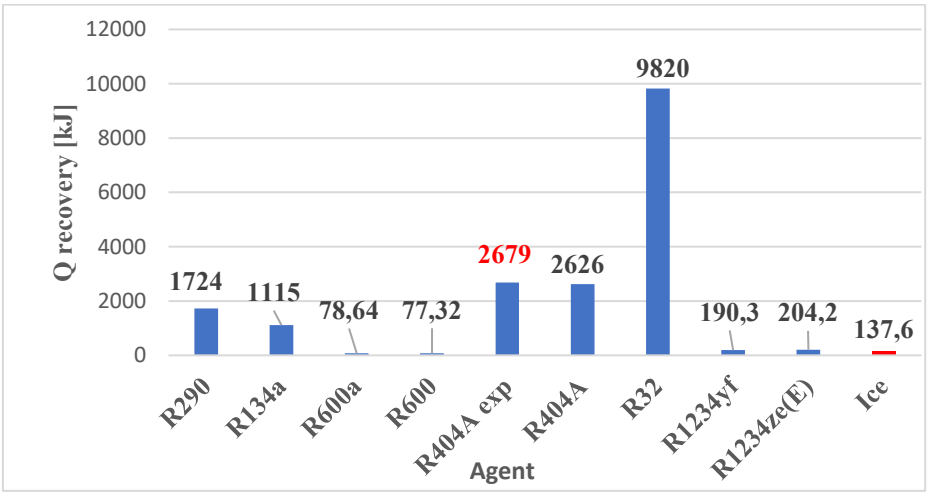


Figure 6.11. shows the Q recovery for all refrigerants.

From Figure 6.11, it can be observed that in terms of supplying thermal energy through recovery and storage, refrigerant R32 stands out significantly, followed by R404A, R290, and R134a.Both in terms of temperature level and the amount of heat recovered and stored, refrigerant R32 is the most suitable for defrosting with PCM-SP50 (see Figures 6.11) followed by R404A, R290, and R134a). The amount of heat required to melt the 400 g of ice deposited on the evaporator in the experimental determinations from Chapter 4 is 137.6 kJ. From this point of view, refrigerants R1234yf and R1234ze(E) can also provide this amount of heat, but not at the temperature required for melting the PCM SP50.

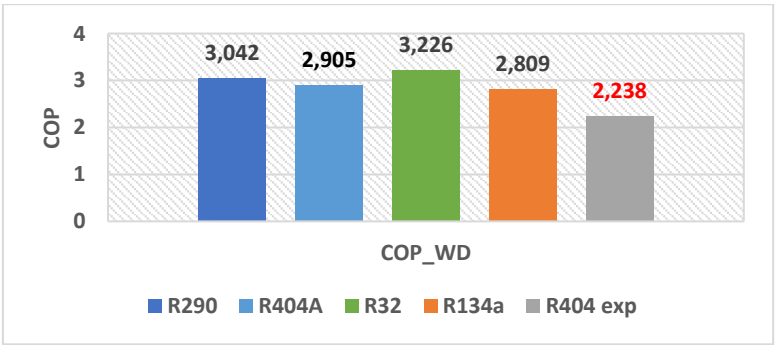


Figure. 6.12 COP for air defrost method

Figure 6.12 shows the Coefficient of Performance (COP) calculated with eq. (6.3) for the air defrosting method using various refrigerants. Under these operating conditions, refrigerant R32

stands out as the refrigerant with the highest energy efficiency. Refrigerant R290 has a good COP, close to that of R32, making it attractive, especially considering its low GWP but it is flammable. Refrigerants R404A and R134a have lower but comparable values (below R290 and R32).

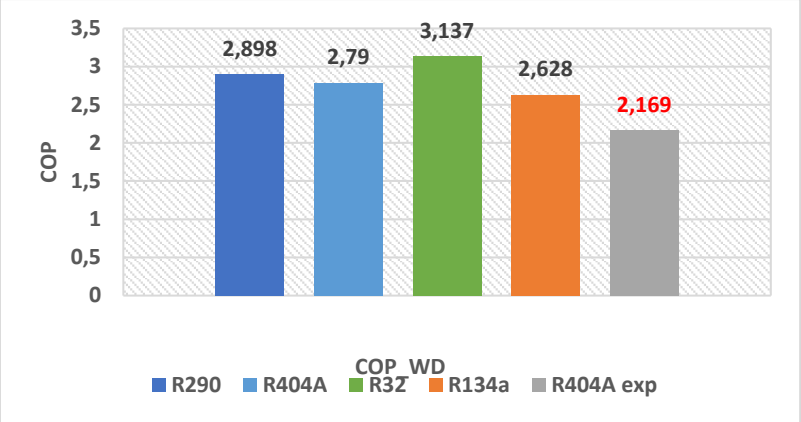


Figure 6.13. COP for electric defrost method

In Figure 6.13, corresponding to the electric heating defrosting method, it is noticed that R32 remains the absolute leader in energy efficiency, R290 has a COP close to 2.9, which confirms good performance, while R404A and R134a show moderate efficiencies, below R290 and clearly below R32. The experimental value for R404A is lower for the same reason mentioned earlier. From Figure 6.13. It can be observed that the COP decreased by approximately 10% compared to air defrosting.

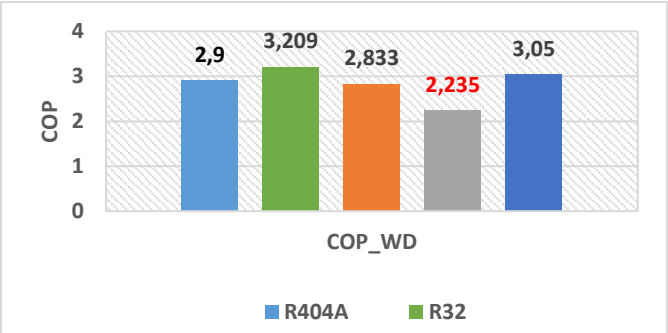


Figure 6.14 COP for hot gas defrost method

In Figure 6.14, for hot gas defrosting, it can be observed that the same hierarchy is maintained for the refrigerants used, with R32 having the highest COP, followed by R290. Refrigerants R404A and R134a remain in the range of 2.8–2.9.

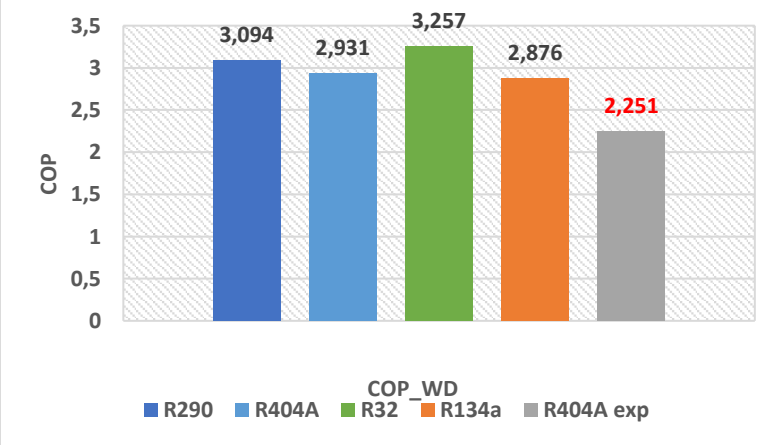


Figure 6.15 COP for PCM defrost method

In Figure 6.15, for PCM defrosting, it can be observed that the same hierarchy is maintained for the refrigerants used, with R32 having the highest COP, followed by R290, R404A and R134a. In conventional studies on the performance of VCRS only the cooling operating mode is considered, while the defrost operating mode is neglected. To enable a comparison between the performance of VCRS with and without defrost, the **COP no-defrost cycle** was defined. This coefficient was determined for each refrigerant using eqs. (6.2), (6.5), (6.8), and (6.11).

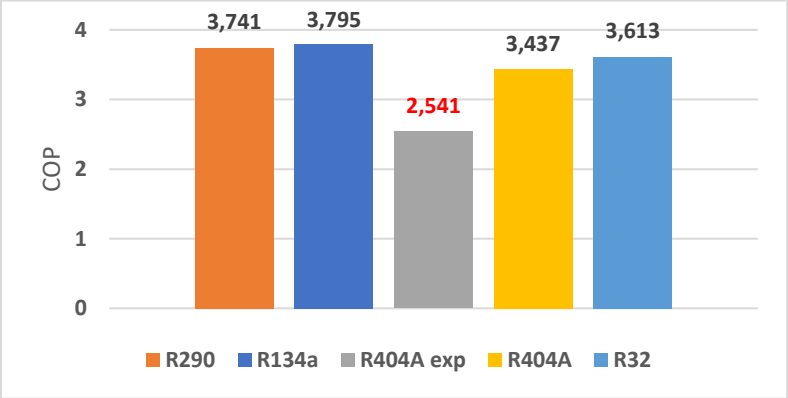


Figure 6.16. No defrost cycle COP

As shown in Figure 6.16, it is observed that R134a and R290 have the highest value, while the lowest value is exhibited by R404A and R404A exp.

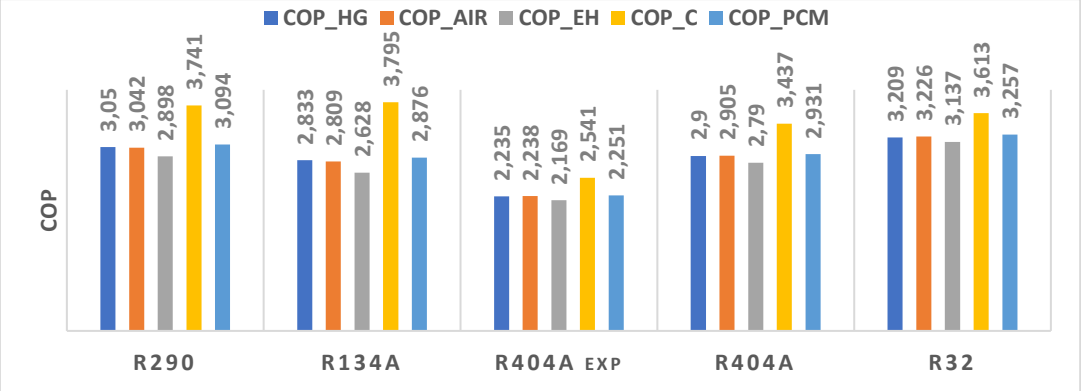


Figure 6.17. Comparative COP - Air defrosting, Electric Heating defrosting, Hot gas defrosting, PCM defrosting and Cycle COP

Figure 6.17 presents a comparison between the four defrosting methods, where it can be observed that the highest COP is achieved by the refrigerant R32 in PCM defrosting, followed by COP in air defrosting, COP in gas defrosting and the lowest value is observed in electric heating defrosting.

From Figure 6.17 it can be noticed that for all considered refrigerants the lowest COP value is obtained for the electric heating defrost method. It can be noticed too that for all considered refrigerants the highest COP value is obtained for the PCM defrost method. For the refrigerants R134a and R290, it is observed that hot gas defrosting method has a higher COP than air defrosting method, with values that are very close to each other. In contrast, for the other refrigerants, the COP of hot gas defrost is lower than that of air defrost.

Chapter 7
Conclusions and personal contributions

C.1. General conclusions

The main objective of the work is to analyze from a theoretical point of view the possibility of increasing the efficiency of the VCRS by implementing a defrosting system with PCM.

The secondary objectives are the following:

-experimental estimation of the amount of ice deposited on the evaporator of the given VCRS;

- establishing experimentally the type of PCM suitable to accumulate thermal energy from the gases discharged by the Cp of the VCRS and its use in the defrosting system of the EV of the VCRS.

- analysis of the influence of the different defrosting systems (air, electric heater, hot gas) including the one with PCM on the global COP for VCRS.

Chapter 1 shows the increasing demand for refrigeration systems, combined with rapid technological advancements, which has significantly contributed to a rise in global energy consumption, resulting in increased emissions of toxic gases and global warming. It is essential to understand the components and operation of vapor-compression refrigeration systems (VCRS) to understand the way to develop the efficiency of each part to reduce the effect on the environment and global warming. Globally the VCRSs are important energy consumers. One of the interesting strategies for enhancing the installation's performance is to minimize energy consumption during the defrost stage.

In **Chapter 2** a literature review regarding methods to enhance the efficiency of VCRs is conducted. The integration of Phase Change Materials (PCMs) into refrigeration systems (RS) offers a promising choice for enhancing system performance, energy efficiency, and temperature control.

Research has demonstrated that incorporating PCMs in refrigeration units can lead to extended refrigeration times, improved temperature distribution, energy savings, and system resilience. By leveraging the latent heat storage capacity of PCMs, refrigeration systems can achieve more efficient cooling, reduce energy consumption, and enhance operational reliability. The customizable nature of PCMs allows for tailored solutions to meet specific refrigeration system requirements, making them a versatile and effective option for optimizing refrigeration processes. Overall, the addition of PCMs in refrigeration systems represents a valuable strategy for improving cooling efficiency, reducing energy costs, and enhancing the overall performance of refrigeration units.

Chapter 3 shows the effect of using PCM heat storage for defrosting the evaporator of a refrigeration system using different refrigerants. The impact of various refrigerants and system parameters on the energy performance of PCM-based defrosting was investigated under the same working conditions.

It was observed that as the defrosting time increases, the refrigerant flow rate required for PCM-based defrosting decreases. Among the refrigerants analyzed, R600 exhibited the lowest mass flow rate, while R404A the highest in order to defrost the same mass of ice. Additionally, the $COP_{with\ pump}$ of the refrigeration system with PCM-based defrosting increases gradually with defrosting time, but it remains slightly lower than the system without defrosting, having comparable values in both cases.

The results indicate that an increase in the evaporating temperature leads to a decrease in the recoverable heat. However, for evaporating temperatures between -10°C and -40°C, the

recoverable heat is sufficient to achieve complete defrosting of the ice accumulated on the evaporator. In contrast, an increase in the condensing temperature improves the amount of recoverable heat for dry and wet refrigerants such as R32, R404A, R134a, and R290, but reduces it for isentropic refrigerants, including R600a, R600, R1234yf, and R1234ze(E).

Superheating plays a critical role in enhancing heat recovery. A higher superheating degree significantly increases the recoverable heat, making PCM-based defrosting viable for isentropic refrigerants. Contrarily, the desuperheating degree varies with condensing temperature: it increases for R32, remains nearly constant for group b) refrigerants, and decreases for group c) refrigerants. This suggests that increasing the condensing temperature can influence the defrosting process differently depending on the refrigerant. Previous analysis reveals that R32 is the most suitable refrigerant for PCM-based defrosting, followed by refrigerants in groups b) and c).

Additionally, the refrigerant quality at state 7 (outlet of the PCMhx during defrosting) has a minimal influence on $COP_{with\ pump}$, with the highest value recorded for R600. As the refrigerant quality increases, the refrigerant mass flow rate required for defrosting decreases, resulting in lower power input for the circulation pump.

Defrosting plays an important role in reducing energy consumption, a conclusion drawn in **chapter 4** from the experimental determinations carried out on the experimental test rig in the Department of Thermodynamics, Engines, Thermal and Refrigeration Equipment, Faculty of Mechanical and Mechatronic Engineering, National University of Science and Technology POLITEHNICA Bucharest. The experimental data obtained are essential for the final analysis regarding the use of a PCM-based system for defrosting, an analysis that is presented in Chapter 6 of this work.

The experimental results show that the ice accumulated in the evaporator is 0,400 kg (Table 4.14). The ice is accumulated on the evaporator during approximately 3,5 h of operation of VCRS with Eclectic Defrost Mode and approximately 3,13 h with Air Defrost Mode.

Experimental results show that air defrosting requires a longer time (26 minutes versus 15 minutes) due to the lower thermal availability of air compared to electric defrost. As a result, the operating time of the system in cooling mode is shorter in the case of air defrosting (188 minutes versus 208 minutes), which has implications for functional parameters.

The evaporator pressure at the end of the defrosting period is higher in the case of electric defrosting than in air defrosting (9 bar versus 7 bar).

It can be observed that the condensing pressure is not significantly influenced by the type of defrosting. This may be explained by the fact that it is controlled by the fan pressure switch. However, it is worth noting the increase of approximately 0.8 bar, from 16 bar to 16.8 bar, in the case of electric defrosting at the beginning of the Ia-System startup period.

The superheating temperature decreases from an average of -3.6 °C for electric resistance defrosting to a minimum of -7 °C (Figure **4.26a**) versus air defrosting where, the average superheating temperature drops from -3.4 °C to a minimum of -7.4 °C (Figure **4.26b)**. This indicates that in both scenarios, ice deposition impairs heat transfer, leading to a reduction in the degree of superheating during the cooling mode cycle.

For the experimentally studied regimes in both cases-electric defrosting (a) and air defrosting (b)-the average discharge temperatures are notably high, measuring 65.9 °C for electric defrosting and 66 °C for air defrosting. These temperatures support the feasibility of PCM defrosting in these operational modes (Figures 4.27a and 4.17b). The same increasing trend in discharge temperature is observed immediately after starting the installation in zones a and b. During the defrosting period, however, there is a decreasing trend, as the discharge pipe cools down to a temperature of 30-35 °C, which is influenced by the ambient temperature.

In System startup-period (area I-a, Figure 4.24.b, 4.30a and 4.30b), the power consumed by the compressor is lower in electric defrosting mode than in air defrosting mode until the system reaches a stable operating condition. However, the average power consumed by the compressor in

both situations is approximately the same, 484 W for electric defrosting and 482 W for air defrosting.

The system utilizing electric defrosting consumes more energy than the one using air defrosting. Specifically, the energy consumption for the electric defrosting system is 2.6 kWh, compared to 2.4 kWh for the air defrosting system, resulting in a difference of approximately 8%. This discrepancy can be attributed to the electric resistance, which consumes about seven times more energy than the fan. Although the electric resistance operates for half the time of the fan during the defrosting period, the total energy consumption throughout an entire refrigeration-defrosting cycle remains higher for the electric defrosting system than for the air defrosting system (Figures 4.32a and 4.32b).

Chapter 5 shows the effect of the inlet temperature and the flow rate on the melting and solidification for PCM using a vertical shell and tube heat exchanger.

The effect of inlet temperature:

Higher inlet temperatures significantly increase the melting rate of PCMs, which is important for optimizing thermal energy storage systems. As the inlet temperature rises, the liquid fraction of the PCM also increases, resulting in a shorter total melting time.

Flow Rate Variations:

The flow rate of the heat transfer fluid (water) significantly impacts heat transfer efficiency and the melting and solidification rates of phase change materials (PCMs). Generally, increasing the flow rate enhances heat transfer, which can speed up the melting process.

Melting and Solidification Dynamics:

The study indicates that during the initial phase of melting, conduction is the dominant mechanism; however, as the PCM transitions to a viscous state, convection becomes more significant. This transition highlights the importance of understanding conduction and convection in PCM applications.

The heat transfer in the vertical tube has a complex nature due to the upward movement of the melted PCM. This phenomenon promotes the rapid melting of the PCM at the top of the VSTHX.

The experiment underscores the importance of optimizing inlet temperature and flow rate to enhance PCM performance in thermal energy storage applications.

The average temperature provides important information in this regard. In the heat accumulation period, the melting temperature is reached first in the base section, section 1 (the bottom of the tube), then "surprisingly" the next section where melting occurs is on level 5, at the top of the tube (Figure 5.15). Melting continues level 2 towards the base then on level 4 towards the end of the tube. The section where melting occurs at the latest is section 3 in the middle of the tube. The process is not surprising if we take into account the two hypotheses mentioned: a high rate of heat transfer by conduction along the outer tube, and an upward gravitational movement of the melted and superheated paraffin, which promotes the melting of paraffin in the upper sections 4 and 5.

Using a water flow rate of 65 ºC accelerates the melting process of the paraffin (Figure 5.16). In the base section, the melting is initiated after 26 minutes compared to 48 minutes when using a water flow of 60 ºC. The melting is also completed in the median section after 64 minutes compared to 110 minutes when using a water flow of 60ºC.

It is observed that as the water temperature increases, the initiation and completion of the melting process is faster, and the melting interval is shorter.

Chapter 6 shows that the defrosting process reduces the cycle COP, regardless of the defrosting method applied, when compared to operation without defrosting. Among the investigated techniques, PCM-based defrosting exhibits the highest coefficient of performance, whereas electric resistance defrosting results in the lowest values. As anticipated, defrosting modifies the coefficient of performance, leading to a depreciation of the cycle COP, which is lower when defrosting is present, regardless of the defrosting method and refrigerant used.

There are refrigerants for which air defrosting is more efficient than hot-gas defrosting (see R32 and R404A), but it has the disadvantage of not completely defrosting the entire ice quantity, leading to increased humidity in the cooled space.

There are refrigerants for which hot-gas defrosting is more efficient than air defrosting (see R290 and R134a), but it leads to increased compressor wear and, consequently, higher operating costs. Both the refrigerant and the defrosting method can modify the overall optimum coefficient of performance provided by the cycle.

Theoretically, the PCM-based defrost cycle achieves the highest COP; however, its implementation involves high costs due to the complexity of the system, making it prohibitive for very small-capacity VCRS installations. Conversely, for medium-capacity refrigeration systems (ranging from 2 kW to 50 kW), PCM defrosting appears to be a viable solution, as it eliminates the disadvantage of premature compressor wear typically associated with hot-gas defrosting.

For R32 and R404A, the second-highest COP value is obtained for air defrosting.

For R290 and R134a, hot-gas defrosting yields the highest COP. Electric defrosting is the weakest in terms of COP.

The mathematical model applied to the experimental results from Chapter 4 confirms the results obtained from the theoretical cycle for the refrigerant R404A, namely that the highest COP is achieved for PCM, air, hot-gas, and electric defrosting.

C.2. Original contribution

The original contribution of this PhD thesis lies in the theoretical and experimental study of using Phase Change Materials (PCMs) for defrosting in Vapor Compression Refrigeration Systems (VCRS). The research introduces innovative methods to enhance the energy efficiency of refrigeration systems by recovering waste heat from compressor discharge gases and storing it in PCMs for defrosting purposes. This approach aims to reduce energy consumption and heat emissions to the refrigerated enclosure during the defrosting process.

Key contributions include:

1. **Outcomes**
2. **Original contributions**

Outcomes

- Mathematical model for VCRS with Air Defrost (subchapter 6.2.1)
- Mathematical model for VCRS with Electric Heater Defrost (subchapter 6.2.2)
- Mathematical model for VCRS with Hot Gas Defrost (subchapter 6.2.3)
- Mathematical model for VCRS with PCM Defrost (Chapter 3)
- The experimental setups from Chapter 4 and Chapter 5
- The experimental data obtained for the two experimental setups in Chapters 4 and 5.

Original contributions

- The PCM defrosting scheme (Chapter 3, Figure 3.1)
- PCM defrosting increases the COP regardless of the type of PCM

For the group c) of refrigerants – the isentropic ones, PCM defrosting cannot be carried out without an increase in the degree of superheating before the compressor inlet, regardless of the PCM type.

- For the refrigerants studied—R290, R134a, R404A, and R32—at a superheating degree of approximately 10.67 °C for Electric Defrost, the highest value of COP is obtained for PCM defrosting and Electric Defrost for R32.
- For R32 and R404A, the second-highest COP value is obtained for air defrosting.
- For R290 and R134a, hot-gas defrosting yields the highest COP. Electric defrosting is the weakest in terms of COP.
- The mathematical model applied to the experimental results from Chapter 4 confirms the results obtained from the theoretical cycle for the refrigerant R404A, namely that the highest COP is achieved for PCM, air, hot-gas, and electric defrosting.
- The energy consumption for the VCRS (0–4 °C) with electric defrosting is 8% higher than with air defrosting (In Chapter 4, Figure 4.32 a,b).
- Experimental determination of the temperature profile during the melting of PCM SP50 when using hot water (60°C, 65°C, 70°C) (In Chapter 5, pg.96).

Overall, the thesis contributes to the field of refrigeration by proposing a sustainable and energy-efficient defrosting solution, supported by theoretical modeling and experimental validation. This innovative approach has the potential to reduce energy consumption and environmental impact in refrigeration systems.

C.3. Future research directions

The PhD thesis on the use of Phase Change Materials (PCMs) for defrosting in Vapor Compression Refrigeration Systems (VCRS) opens up several avenues for future research. These directions aim to further enhance the efficiency, applicability, and sustainability of PCM-based defrosting systems. Key future research directions include:

Exploration of Alternative PCMs:

- Investigate new PCMs with lower melting points, higher latent heat storage capacities, and improved thermal conductivity to optimize heat recovery and defrosting efficiency.
- Develop advanced composite PCMs with enhanced thermal properties to reduce melting and solidification times.

Integration with Renewable Energy Sources:

Study the integration of PCM-based defrosting systems with renewable energy sources, such as solar or wind energy, to further reduce the environmental impact and reliance on conventional energy sources.

Application in Large-Scale Refrigeration Systems:

Extend the research to larger refrigeration systems, such as those used in industrial and commercial applications, to evaluate the scalability and economic feasibility of PCM-based defrosting.

Advanced Heat Exchanger Designs:

- Explore innovative designs for PCM heat exchangers to improve heat transfer efficiency and reduce thermal resistance.
- Investigate the use of nanotechnology to enhance the thermal conductivity of PCM containers and heat exchangers.

Economic Analysis:

- Perform detailed cost-benefit analyses to evaluate the economic feasibility of PCM-based defrosting systems in various applications.
- Investigate the potential for cost reduction through mass production and material optimization.

Environmental Impact Assessment:

- Assess the environmental benefits of PCM-based defrosting systems, including reductions in CO2 emissions and energy consumption.
- Explore the use of eco-friendly refrigerants in combination with PCM-based defrosting systems.

Energy Recovery from Other Sources:

- Explore the possibility of recovering waste heat from other components of the refrigeration system, such as the condenser, to enhance the overall energy efficiency.

By addressing these future research directions, the potential of PCM-based defrosting systems can be further realized, contributing to the development of more sustainable and energy-efficient refrigeration technologies.

Published articles

1. **Jamal AL DOURI**, Kamel S. HMOOD, Valentin APOSTOL, Horatiu POP, Saleh J. ALQAISY, and Elena Beatrice IBREAN, "Literature review regarding defrosting methods for household refrigeration", 10th International Conference on Thermal Equipment, Renewable Energy and Rural Development, TE-RE-RD 2021, E3S Web of Conferences **286**, 01012 (2021), doi.org/10.1051/e3sconf/202128601012).
2. **J AL Douri**, H Pop, V Apostol, N K Fadhil, K S Hmood, S J AL Qaisy, A Nabbat, C Ionita and T Prisecaru, "Preliminary experimental assessment of a vertical shell and tube heat exchanger based on phase change materials. IOP Conference Series: Materials Science and Engineering, Volume 1262, The 10th International Conference on Advanced Concepts in Mechanical Engineering (ACME 2022) 09/06/2022 - 10/06/2022 Online
3. A L Tarish, **J Al Douri**, V Apostol2, H L Pop2 and C Ionita" Exergy and performance analyses of impact subcooling for vapor compression refrigeration system utilizing eco-friendly refrigerants". IOP Conference Series: Materials Science and Engineering, Volume 997, The 9th International Conference on Advanced Concepts in Mechanical Engineering - ACME 2020 4-5 June 2020, Iasi, Romania
4. **Jamal AL DOURI**, Valentin APOSTOL, Horatiu POP, Tudor PRISECARU, Cornel Constantin PAVEL, Iulian UTA, Claudia IONITA, "Improving performance of cold room refrigeration system by desuperheating energy recovery using PCMs" INMATEH Agricultural Engineering, Vol. 70, No. 2 / 2023, DOI: https://doi.org/10.35633/inmateh-70-53.

Selective Bibliography

[1] R. Rybár, D. Kudelas, and M. Beer, "Selected problems of classification of energy sources – What are renewable energy sources?," *Acta Montan. Slovaca*, vol. 20, no. 3, pp. 172–180, 2015.

[2] F. Nadeem, S. M. S. Hussain, P. K. Tiwari, A. K. Goswami, and T. S. Ustun, "Comparative review of energy storage systems, their roles, and impacts on future power systems," *IEEE Access*, vol. 7, pp. 4555–4585, 2019.

[17] C. Park, H. Lee, Y. Hwang, and R. Radermacher, "Recent advances in vapor compression cycle technologies," *Int. J. Refrig.*, vol. 60, pp. 118–134, 2015.

[18] S. P. Chavhan and P. S. D. Mahajan, "A Review of an Alternative to R134a Refrigerant in Domestic Refrigerator," vol. 3, no. 9, 2013.

[51] M. Amer and C. C. Wang, "Review of defrosting methods," *Renew. Sustain. Energy Rev.*, vol. 73, no. December 2015, pp. 53–74, 2017.

[52] J. Al Douri, K. S. Hmood, V. Apostol, H. Pop, S. J. Alqaisy, and E. B. Ibrean, "Review regarding defrosting methods for refrigeration and heat pump systems," *E3S Web Conf.*, vol. 286, pp. 1–13, 2021

[86] S. E. Hosseini and M. A. Wahid, "Hydrogen production from renewable and sustainable energy resources: Promising green energy carrier for clean development," *Renew. Sustain. Energy Rev.*, vol. 57, pp. 850–866, 2016.

[87] P. S. Raveendran and S. J. Sekhar, "Performance studies on a domestic refrigerators retrofitted with building-integrated water-cooled condenser," *Energy Build.*, vol. 134, pp. 1–10, 2017.

[121] H. Ge, H. Li, S. Mei, and J. Liu, "Low melting point liquid metal as a new class of phase change material: An emerging frontier in energy area," *Renew. Sustain. Energy Rev.*, vol. 21, pp. 331–346, 2013.

[122] A. Sharma, V. V. Tyagi, C. R. Chen, and D. Buddhi, "Review on thermal energy storage with phase change materials and applications," *Renew. Sustain. Energy Rev.*, vol. 13, no. 2, pp. 318–345, 2009.

[167] Jamal Al Douri, Adrian Chiriac, Tudor Prisecaru, Horatiu Pop, Valentin Apostol, Claudia Ionita, Comparison between defrosting methods using different refrigerants, UPB Scientific Bulletin, Series D: Mechanical Engineering Vol. 86, Iss. 2, 2024, ISSN 1454-2358

[168] Pop H, Apostol V, Alqaisy S J, Hmood K S, Al Douri J And Badescu *V* 2021, Mass flow rate evaluation of a hermetic compressor from a small scale vapour compression refrigeration system, UPB Scientific Bulletin, Series D: Mechanical Engineering 83 pp 1454-2358.

[171] Jamal al Douri, V. Apostol, H Pop, T. Prisecaru, C. C, Pavel, I. Uta, C. Ionita, L. Popa, Improving performance of cold room refrigeration system by desuperheating energy recovery using PCMs, doi: https://doi.org/10.35633/inmateh-70-5